Sustainable Structures
ISSN: 2789-3111 (Print); ISSN: 2789-312X (Online)
http://www.sustain-dpl.com/journal/sust
DOI: 10.54113/j.sust.2026.000095

REVIEW ARTICLE

Bond of steel and FRP reinforcement in recycled aggregate concrete: a critical review

Thanongsak Imjai [a,*], Radhika Sridhar [b], Hongguang Wang [c], Reyes Garcia [d], U. Johnson Alengaram [e], Radhakrishna G Pillai [f]

[a]Department of Civil Engineering, Faculty of Engineering, Burapha University, Chonburi 20131, Thailand
[b]School of Engineering and Technology, Walailak University, Nakhon Si Thammarat 80160, Thailand
[c]College of Aerospace and Civil Engineering, Harbin Engineering University, Harbin 150001, China
[d]Built Environment & Sustainability Cluster, School of Engineering, University of Warwick, Coventry, CV4 7AL, UK.
[e]Department of Civil Engineering, Faculty of Engineering, Universiti Malaya, 50603, Kuala Lumpur, Malaysia
[f]Department of Civil Engineering, Indian Institute of Technology Madras, Chennai 600 036, India
*****Correspondence: thanongsak.im@eng.buu.ac.th

Abstract: The use of recycled concrete aggregates (RCA) in recycled aggregate concrete (RAC) presents a solution to reduce dependence on raw natural resources. However, the bond behaviour of reinforcing bars embedded in RAC is challenging, mainly due to contradictory results in literature. This critical review examines the mechanisms influencing bond strength of steel and fibre reinforced polymer (FRP) reinforcement in RAC, emphasising key factors such as surface roughness, interaction at the interfacial transition zone (ITZ), and the concrete's properties. Additionally, the review discusses the main differences in bond performance between FRP reinforcement and normal steel bars, highlighting the FRP bars' reliance on adhesion and friction, rather than mechanical interlocking. Various testing methods in line with current standards are discussed, alongside relevant design equations from European and North American guidelines for anchorages and lap splices. It is found that moderate RCA replacement levels (50%-75%) can improve the bond strength of bars due to a rougher interfacial transition zone. However, high levels of RCA replacement (~100%) can reduce bond strength by up to 38%. Current design codes primarily focus on steel and FRP reinforcement embedded in normal concrete, and therefore these should be revised to extend their applicability to RAC elements to promote the faster adoption of RAC in engineering practice. Future research needs are also provided. This study contributes towards a better understanding of bond behaviour of reinforcement in RAC, which in turn is expected to facilitate the broader adoption of circular economy practices in construction.

Keywords: bond strength, fiber-reinforced polymer, recycled aggregate, pull-out test, anchorages, Tepfer's model

1 Introduction

Amid the climate emergency and resource depletion challenges, various strategies have been adopted to address these environmental threats [1]. For example, in 2015, the Paris Agreement set targets to reduce greenhouse gas emissions, while the European Union pledged to achieve carbon neutrality by 2050, aiming to decouple economic growth from the consumption of natural resources.

Received: 14 February 2025; Received in revised form: 6 May 2025; Accepted: 29 August 2025

Similarly, China has committed to carbon neutrality by 2060, focusing on green, resource-efficient development and shifting towards the adoption of more sustainable materials in construction [2].

A potential solution to minimise the depletion of natural resources is the incorporation of recycled concrete aggregates (RCA) derived from demolished buildings in the production of recycled aggregate concrete (RAC) [3]. By utilising RCA, the pressure on natural aggregate supplies can be reduced, while also helping to decrease the volume of construction and demolition (C&D) that is disposed in landfills [4]. In addition, RAC promotes the adoption of circular economy principles by lowering the environmental impact of building materials [5].

1.1 Background on RAC and significance

Since the early 1900s, concrete has been the primary material in construction, becoming an essential component of the industry [6]. Nevertheless, it contributes to nearly 8% of worldwide carbon dioxide emissions. Urbanisation and infrastructure development increase the need for concrete, as well as for aggregates which make up 70-80% of concrete's total volume. The demand for natural aggregates is approximately 48.3 billion tons per year, with a growth rate of 5% every five years [7]. This demand is expected to double in the coming decades, thus intensifying the pressure on already scarce natural resources. The generation of C&D waste is also a pressing concern in many regions. C&D waste includes materials generated during the construction, renovation, or demolition of buildings, although most of it is concrete. In 2018, China, the USA, India, and the United Kingdom generated millions of tons of such C&D waste, with China being the largest producer. Inadequate disposal methods for C&D waste contribute to environmental pollution and place increasing demands on landfills [8]. For instance, in 2013, landfills in China accumulated over 7.5 billion cubic meters of C&D waste. This growing waste problem has prompted governments, industries, and academic institutions to invest in recycling and reusing C&D waste materials. Historically, C&D waste has been downcycled for non-structural uses like garden pavements or gabions, but these applications remain limited compared to the volume of waste generated.

Over the past 70 years, research has shown that substituting natural aggregates with recycled aggregates in concrete can reduce material costs by 10-20% [9]. For instance, the Netherlands successfully implemented RAC in over 60% of infrastructure projects. Additionally, life cycle assessments of RAC (e.g. as those conducted in Hong Kong) showed important environmental benefits, such as reductions of greenhouse gas emissions (up to 65%) and of non-renewable energy consumption (up to 58%) compared to using conventional natural aggregate concrete (NAC) [10]. Despite these advantages, the adoption of RAC in structural applications has been hindered by its (often) lower mechanical properties compared to NAC. Although recycling facilities for C&D waste have improved in the last decades, the production and widespread use of RAC has not significantly advanced. Addressing these challenges is crucial to enhance the performance and viability of RAC in the construction industry.

1.2 Significance of bond at reinforcement and concrete/RAC interface

Steel-reinforced concrete is commonly used as a main structural material in construction. The bond between the steel reinforcement and the surrounding concrete is essential in determining the overall performance of reinforced concrete (RC) structures [11]. Reinforced concrete (RC) components in these structures can withstand external loads if sufficient bond strength is developed between the reinforcement and the concrete. When the bond strength and stiffness are sufficient, the two materials deform in harmony without significant slippage between them [12]. Bond strength ensures a seamless load transfer between the reinforcement and concrete, thus transferring loads safely between them and ensuring strain compatibility [13,14]. Generally, the ductile capacity of RC members depends heavily on the bond strength developed between the (steel) reinforcing bars and the surrounding concrete [15].

Bond of steel reinforcement to concrete has been extensively studied in the last 40 years and a bulk of experimental and analytical work has been published on this subject. However, more attention was received after Tepfer's described the bond transfer mechanism between deformed steel bars and NAC [16].

According to Tepfer's theory [16, 17], bond forces are transferred from the bar ribs into the adjacent concrete, creating an angle ‘α’ relative to the pulled bar as shown in **Fig. 1a**. The radial components of these forces are balanced by tensile stresses within a concrete ring surrounding the bar, leading to the formation of internal longitudinal cracks near the bar, as illustrated in **Fig. 1b**. If the concrete cover is thin, longitudinal (splitting) cracks can occur, as depicted in **Fig. 1c**. If the radial stress surpasses the tensile strength of the surrounding concrete, the resistance of the concrete ring diminishes. This results in the steel bar slipping as the splitting cracks extend and widen, eventually causing the concrete ring to fail suddenly in a brittle manner, as shown in **Fig. 1d**.

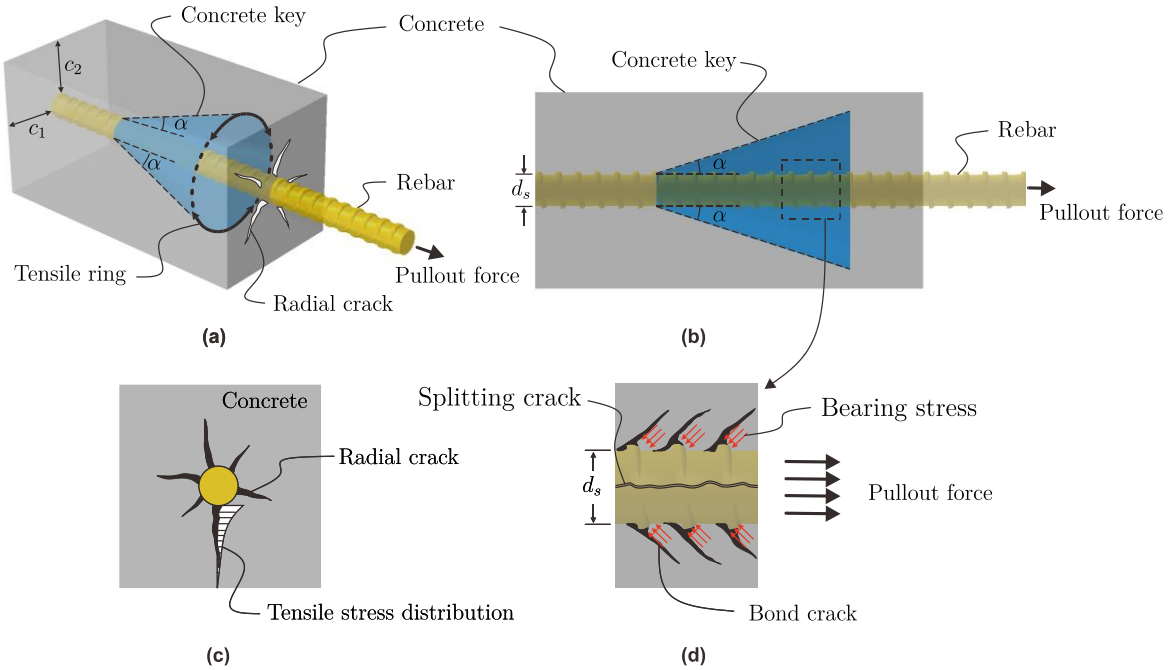

Fig. 1. Tepfer’s theory of bond in an anchored bar: (a) 3D representation of bond mechanism (radial cracking), (b) longitudinal section view (pull-out force), (c) cross-section of the splitting crack formation, and (d) shear and frictional resistance mechanism of the crack (bond cracking).

Much research has been conducted on the bond strength between reinforcing steel bars and natural aggregate concrete (NAC). However, fewer recent studies have focused on the bond characteristics between deformed steel bars and recycled aggregate concrete (RAC). Previous conflicting studies have shown that RAC can either improve or reduce bond strength. In some cases, RAC may enhance bond strength due to the increased roughness from the recycled concrete aggregates (RCA) in the composite material. However, a decrease in bond strength has also been observed, likely due to the lower density of RAC [18-20]. Past studies have also showed that the crushing strength of recycled coarse aggregates and the crack resistance of concrete have a significant impact on the adhesion properties. **Fig. 2** illustrates the normalised bond strength of steel bars for different RCA contents in RAC. Some studies suggest that the use of RCA in concrete does not notably affect the bond between steel reinforcing bars and concrete, with only a marginal reduction of up to 10% compared to NAC [21]. This is likely because the properties of the reinforcement, such as surface texture and rebar type, play a more significant role than the properties of the aggregates. On the other hand, other studies have found that bond strength increases with a higher proportion of RCA in the concrete, as the presence of air voids can decrease the overall strength [22].

The results shown in **Fig. 2** indicate that the normalised bond strength fluctuates considerably with the level of RCA replacement. As seen in **Fig. 2**, the normalised bond strength begins at 0.0138 for 0% RCA replacement (representing NAC) and then decreases slightly to 0.0118 at a 20% RCA replacement. A notable drop is observed at 25% RCA replacement levels, where the normalised bond strength reaches its lowest value of 0.0028, indicating weaker bond at this level. However, with further increases in RCA contents, the bond performance improves, reaching 0.0182 at 50% RCA replacement and stabilising around 0.022 at 75% RCA replacement. This trend suggests that at moderate RCA replacement levels (50% to 75%), the bond efficiency may benefit from the rougher interfacial transition zone (ITZ) of

recycled aggregates. Indeed, the rough surface texture of recycled coarse aggregates (RCA) can lead to improved bond strength by enhancing friction between the rebar and the concrete. Another factor that could enhance bond strength is internal curing, especially when RCA is used in a saturated surface dry (SSD) condition [24]. However, at high levels of 100% RCA replacement, the normalised bond strength slightly decreases to 0.02, suggesting that complete replacement of natural aggregates may reduce overall bond efficiency. This is likely due to the weaker interfacial transition zone (ITZ) characteristics, which compromises bond behaviour.

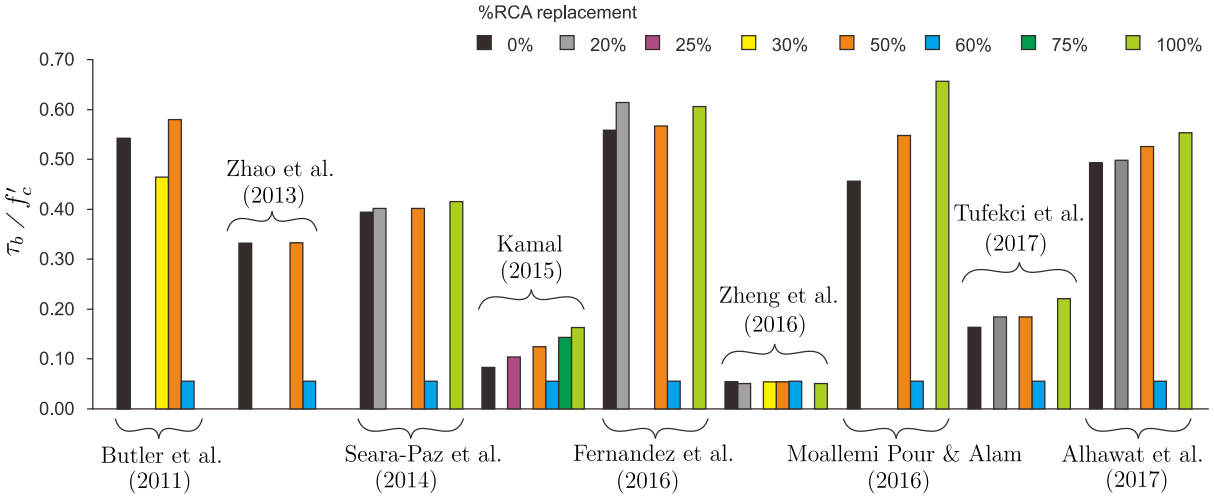

Fig. 2. Comparison of bond strength in terms of RCA replacement levels (adapted from [23]).

In harsh and aggressive environments, the corrosion of steel reinforcement can cause damage or even failure of structural components. To address this limitation, FRP reinforcement has become increasingly popular due to its exceptional corrosion resistance, and remarkable long-term durability in challenging environments. Unlike steel bars where bond relies on mechanical interlocking provided by the ribs, the bond of FRP reinforcement relies primarily on adhesion and friction, which in turn affects bond performance in concrete. Despite numerous studies on the bond strength of steel reinforcement in RAC, limited research has examined the performance of FRP reinforcement in RAC, particularly in terms of its bond mechanisms, influencing factors, and integration into design codes. In RAC, there are additional challenges, as its higher porosity and weaker interfacial ITZs can diminish the bond effectiveness of FRP bars. To improve adhesion, surface treatments like sand coating, ribbing, and the application of chemical bonding agents are commonly used on FRP bars. Additionally, interfacial behaviour differs significantly: whereas steel-concrete bond failures typically involve bar slippage, FRP bond failures are often governed by adhesive failure at the reinforcement-matrix interface (i.e. pull-through failures). Understanding these differences is essential for optimising FRP use in RAC structures, particularly as bond failures often occur in the FRP bar itself, thus making bond strength at the FRP-RAC interface a potential weak link that can lead to structural failures.

This article addresses the above gaps by providing a critical review of the bond behaviour between steel and FRP bars and RAC, focusing on the various parameters that influence bond strength and its characteristics. A comprehensive overview of recent literature is presented, including test methods and relevant codes of practice. Accordingly, this study provides insights to facilitate the broader adoption of FRP in RAC structural applications.

The review examines recent studies as part of a working group (RAC-Thailand) based on various influencing factors, as shown in **Fig. 3**.

Initially, a literature collection and database (step 1) compiled research on bond performance in concrete structures. Databases and experimental studies (step 2) were assessed to analyse bond mechanisms through laboratory testing. Various experimental techniques, such as pull-out tests, beam-end tests and spliced beam tests, are found to be widely adopted to evaluate bond strength in concrete structures. In Step 3, theoretical and analytical bond models were evaluated to examine the accuracy and reliability of predictive equations. The influence of material properties and environmental conditions (e.g. durability, moisture effects) on mechanical performance were evaluated (step 4). To

enhance standardisation, step 5 compared existing design codes and guidelines, identifying discrepancies in design approaches. Finally, step 6 outlined future research directions and novel contributions. This methodology is expected to provide a better understanding of bond behaviour in FRP reinforced RAC elements, thus facilitating its adoption in structural applications.

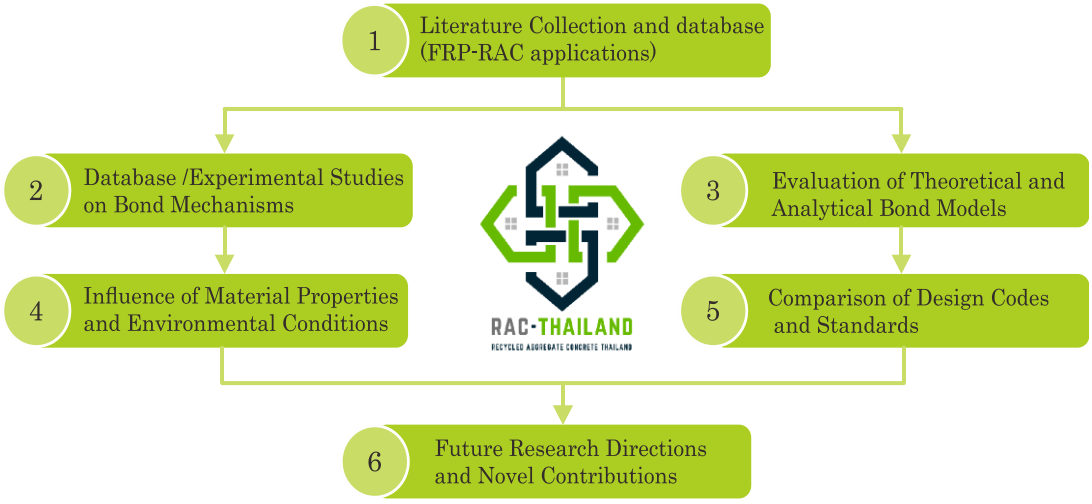

Fig. 3. Flowchart of methodology outline.

2 Overview on recycled aggregate concrete (RAC)

In recent years, RAC has gained widespread attention for a better management of C&D waste [28, 29]. Beyond the environmental benefits, RAC can reduce construction costs and dependence on raw aggregates, thus promoting circular economy principles in construction. **Table 1** summarises recent studies on RAC mechanical properties. A comprehensive review of the properties of RCA and RAC was recently provided by Neupane et al [3].

Table 1. Summary of recent research on properties of RAC

References	Main findings
Verian et al. [30]	The study evaluates the mechanical properties of RAC, covering compressive strength, flexural strength, splitting tensile strength, and elastic modulus
Shi et al. [31]	Study examines enhancement methods on the aggregate from recycled concrete for RAC applications
Liang et al. [32]	Research investigates carbonation mechanisms and technologies to enhance RAC performance
Tam et al. [33]	Study proposes improvements for the microstructural properties of RAC
Liang et al. [34]	Research focuses on the movement of ions that contribute to steel corrosion in RAC

The lower quality of RAC presents a major challenge in substituting natural aggregates with recycled aggregates. As a result, the structural applications of RAC are still somewhat limited. Much of the lower quality of RAC can be attributed to the properties of RCA. **Fig. 4** presents a schematic view of the microstructure of RAC, highlighting key components such as old adhered mortar, fine aggregate, two ITZs (old and new), porosity in both mortars, and cracks in the RCA caused by the recovery process. The weaker microstructure of RAC can be attributed in part to the presence of two ITZ layers present in RCA, as shown in **Fig. 4** [3, 35].

Overall, previous studies suggest that the volume of the interfacial transition zone (ITZ) in RAC is higher than that in NAC due to the adhered mortar, which increases the concrete's porosity and weakens its mechanical properties, such as lower compression strength, splitting tensile strength, and bending resistance [36, 37]. These differences can have significant effects on the corrosion of reinforcement and the deterioration of the concrete. Additionally, the presence of old mortar on recycled aggregates (RA) facilitates the propagation of pre-existing cracks in the mortar under applied loads, reducing the compressive strength of RAC relative to NAC [38]. The compressive strength of RAC can decrease by as much as 7% if the aggregate contains more than 0.05% aluminium impurities in its

chemical composition [39].

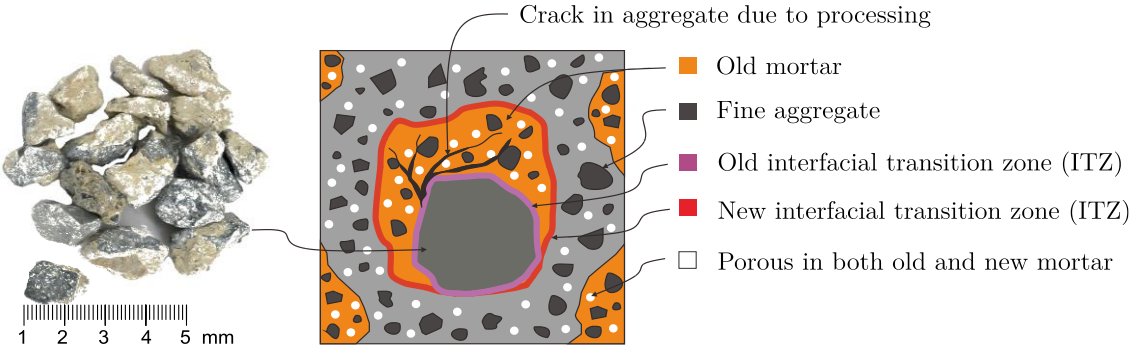

Fig. 4. Microstructural view of RAC (adapted from [3,35]).

Previous studies have utilised atomic force microscopy to evaluate the indentation modulus (EIM) in both the existing and newly formed ITZs between recycled aggregates and fresh mortar in RAC [40]. The findings indicate that the EIM in the ITZ is generally lower than that of both natural aggregates and the mortar matrix. As depicted in **Fig. 5**, the average indentation modulus (EIM) in RAC was found to be between 25 μm and 70 μm lower than those in the ranges of 0 μm to 25 μm and above 70 μm, indicating that the thickness of the interfacial transition zone (ITZ) for the tested aggregate is approximately 45 μm.

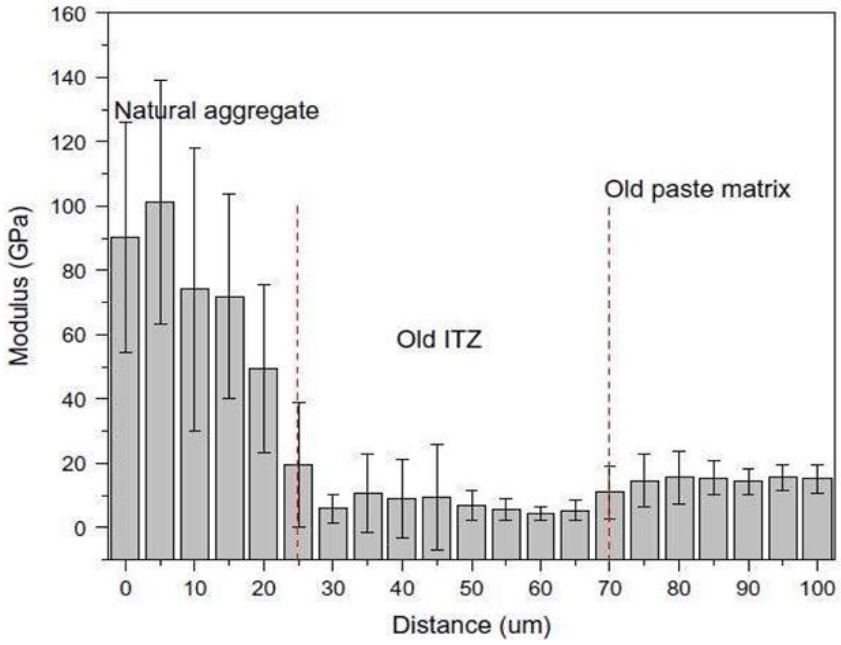

Fig. 5. Indentation modulus through atomic force microscope of ITZ of RAC (adapted from [41]).

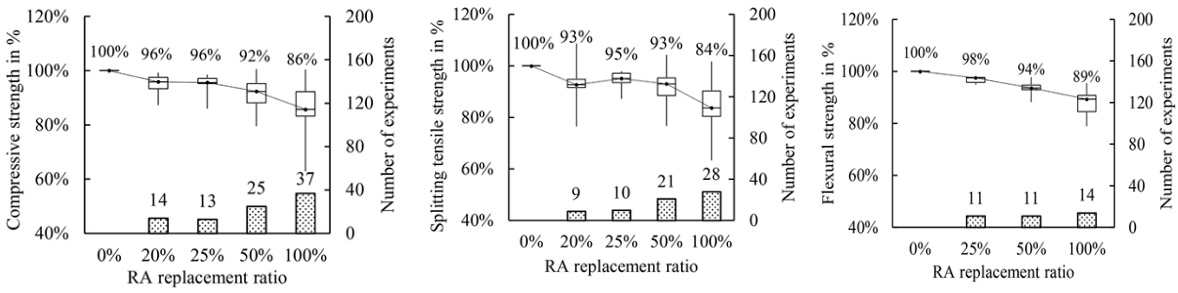

(a) (b) (c)

Fig. 6. Properties of RAC with varying recycled aggregate proportions: (a) compressive strength, (b) split tensile strength, (c) flexural strength (adapted from [47]).

To better understand the behaviour of RAC, it is crucial to compare its mechanical and physical properties with those of NAC in both the fresh and hardened states. The replacement of natural aggregates with RCA in RAC affects several key properties. For instance, fresh RAC mixes typically exhibit lower slump values compared to NAC mixes due to the increased water absorption and rougher (more irregular) surfaces of the recycled aggregates [42, 43]. To achieve similar workability in RAC with a slump range of 100–105 mm, an additional 5%–15% water by volume is required. Additionally, the penetration of aggressive ions in RAC is greater than in NAC, mainly due to the higher permeability, which in turn promotes the cathodic reaction of hydroxyl ions and speeds up the corrosion of steel reinforcement. If 100% recycled aggregates are used in RAC, the relative passed charge can be up to twice as high as in NAC. **Figs. 6a-c** present test results that confirm a reduction in compressive, split (tensile), and flexural strengths of RAC, with average decreases of 40%, 40%, and 20%, respectively, compared to counterpart NAC mixes [46, 47].

Despite the huge potential of RCA in RAC for structural use, its practical application remains limited. Indeed, in real practice, commercial RCA is often downcycled in fillings, road sub-bases and embankments, pavement construction, drainage works and gabion walls [48]. Moreover, RAC is primarily used in non-structural applications, owing to its low load-bearing capacity and inherent variability. As a result, only a limited number of structures have been constructed using RAC. One example of a structural application is the E Science Lab in Switzerland, a 6 storey building with a total floor area of 11,650 m ². Another example is a multi-story residential building in Konan-ku, Yokohama. Similarly, the International Aviation Service Centre in Shanghai was constructed using about 40,000 m ³of RAC [49]. China in particular faces significant challenges in managing C&DW [50, 51] and is therefore a potential supplier of RCA materials. However, factors such as the lack of technical approaches, inadequate off-site recycling support, and insufficient advanced recycling technologies prevent broader adoption of RAC in construction. This issue is also prevalent in other parts of Asia, where structural applications of RAC are being explored despite facing numerous technological and scientific challenges [53, 54].

3 Bond mechanisms of steel and FRP bars

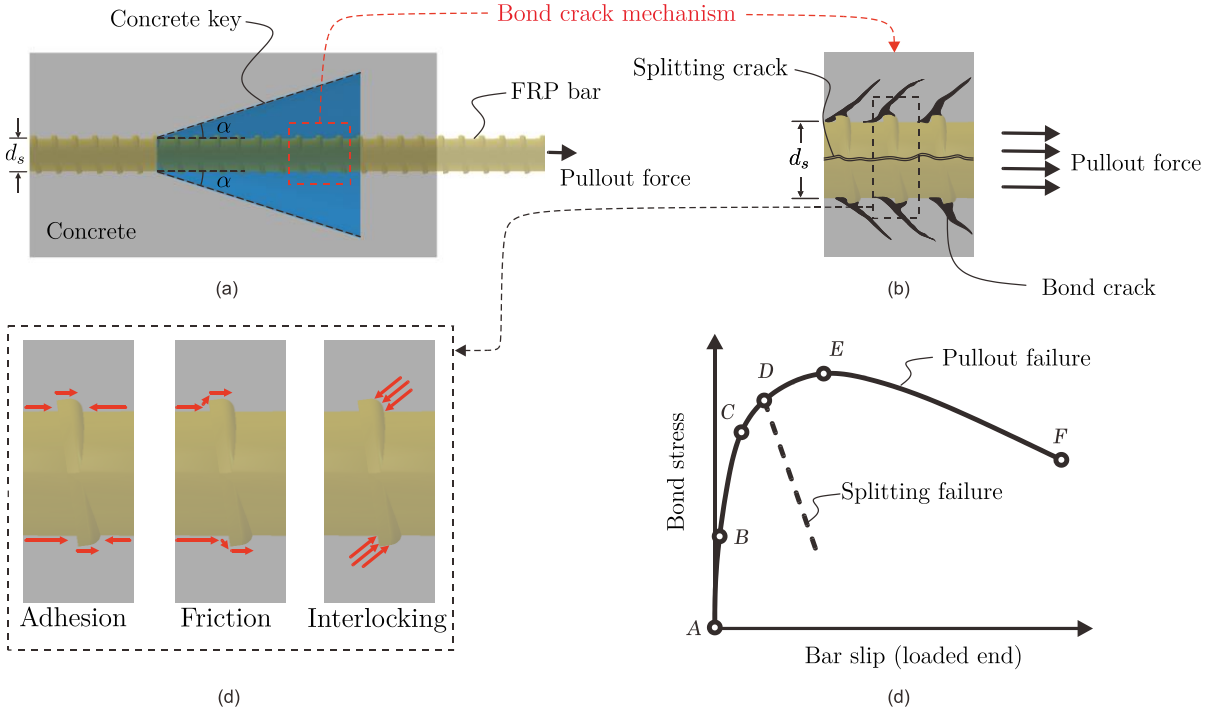

Fig. 7. Bond mechanism between concrete and FRP bar: (a) bond mechanism, (b) splitting crack, (c) bond strength components (adhesion, friction, and interlocking), and (d) bond stress-slip curve (adapted from [56]).

Bond strength describes the interaction between reinforcing bars and the surrounding concrete as bars are pulled by a force [55]. Unlike steel bars, bond of FRP bars relies predominantly on adhesive

and frictional forces due to its smooth surface texture. The bond mechanism of an FRP bar embedded in concrete is illustrated through different stages of load transfer and failure, as shown in **Fig. 7**. The bonding performance of Glass FRP (GFRP) bars is influenced by the interaction between the bar surfaces and the concrete matrix that surrounds them. Unlike steel bars, GFRP bars are more likely to fail via a pull-through mechanism, particularly if the bond strength is insufficient. **Fig. 7a** shows localised stress concentrations around the ribs, leading to concrete cracking. **Fig. 7 (**illustrates splitting cracks along the interface when radial tensile stress exceeds the tensile strength of the concrete, causing bond failure before full a bar pullout failure. Bond strength in GFRP bars is influenced by adhesion, friction, and interlocking (**Fig. 7c**). Adhesion results from chemical bonding, friction arises from surface roughness, and interlocking involves mechanical engagement between the ribs and concrete. Surface treatment, such as sand-coating or ribbing, enhances the bond strength, reducing pull-through failure. The bond stress-slip curve (**Fig. 7d**) reveals the bond strength increasing with slip up to a peak, after which it declines, indicating failure. This suggests that FRP bond performance is governed by mechanical interlocking, friction, and adhesion, with failure modes typically due to concrete cracking or pull-through, influenced by the bar's surface treatment [56].

In conventional steel bars, bond failures are typically caused by rib bearing, leading to concrete splitting or shearing of the concrete keys. In contrast, bond failures in FRP bars often occur due to pull-through mechanisms, as these bars do not rupture the concrete specimen. The bond strength of FRP bars is influenced by multiple factors, including material properties, rib geometry, and surface characteristics. While adhesion and friction are important for bond strength, the rib geometry and surface treatment play critical roles in determining bond performance, as they affect mechanical interlock and resistance to pull-through failure [57]. In contrast to deformed steel bars, where bond strength is mainly influenced by the mechanical interlock of ribs and limited chemical adhesion, the strength is influenced by a combination of rib design, surface roughness, and the properties of the material. These elements are essential in preventing pull-through failure [58, 59]. A visual representation of an FRP slip failure is shown in **Figs. 8a-b**.

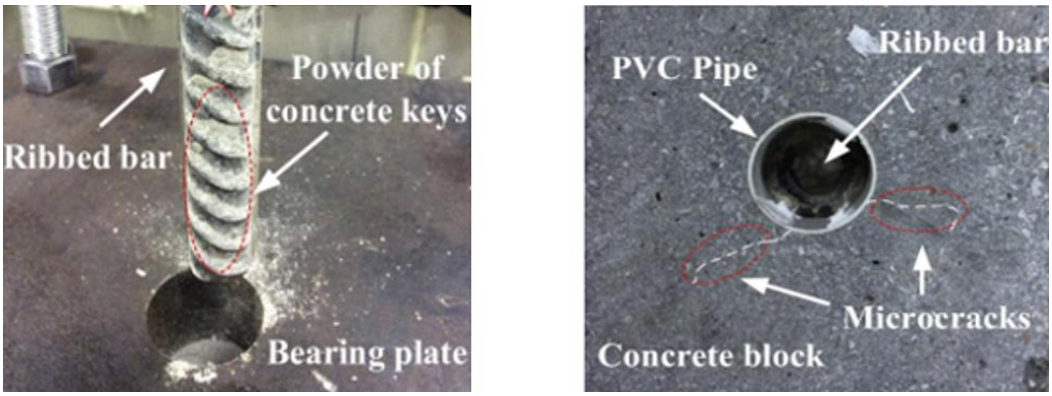

(a) (b)

Fig. 8. FRP bar failure: (a) physical appearance of the FRP bar, (b) SEM image of FRP bond failure. (adopted from [59]).

4 Testing and evaluation methods to study bond behaviour

Bond behaviour can be described using bond stress-slip relationships [60-62]. Bond strength is usually assessed through three common test methods: the pull-out test, the beam end test, and the spliced beam test.

4.1 Pull-out test

The pull-out test has been extensively used to measure bond strength due to its simplicity. This test is also included in EN 10080 [63] for evaluating the bond characteristics of ribbed and indented bars. The pull-out test applies increasing tensile force to one end of a reinforcement bar anchored in a concrete cube, while the other end of the bar remains free. **Fig. 9a** presents a schematic view of the test setup, which includes an actuator that applies tensile force, a load cell for measuring force, a gripping system and housing frame for stability, and a concrete base for structural support. **Fig. 9b** highlights key test

components, bearing plates for load distribution, and a rubber bearing plate to reduce stress concentrations. A rig with linear variable displacement transducers (LVDTs) is positioned to monitor displacement (see **Fig. 9c**), which enables three-point displacement measurement.

The reinforcement bar is usually positioned at the centre of the specimen with an embedment length of five times the bar diameter. To isolate bond action along the rest of the bar, a sleeve is used around it to debond it from the concrete. The bond stress-slip relationship is derived from the applied tensile force and the corresponding slip of the bar until failure occurs. While the stress conditions in the specimen do not fully replicate those in actual concrete members, pull-out tests are valuable for identifying key parameters that influence bond behaviour. However, due to the short anchorage length used in these tests, the results cannot be directly applied to design purposes and are instead used primarily for comparison among bars, or for benchmark testing.

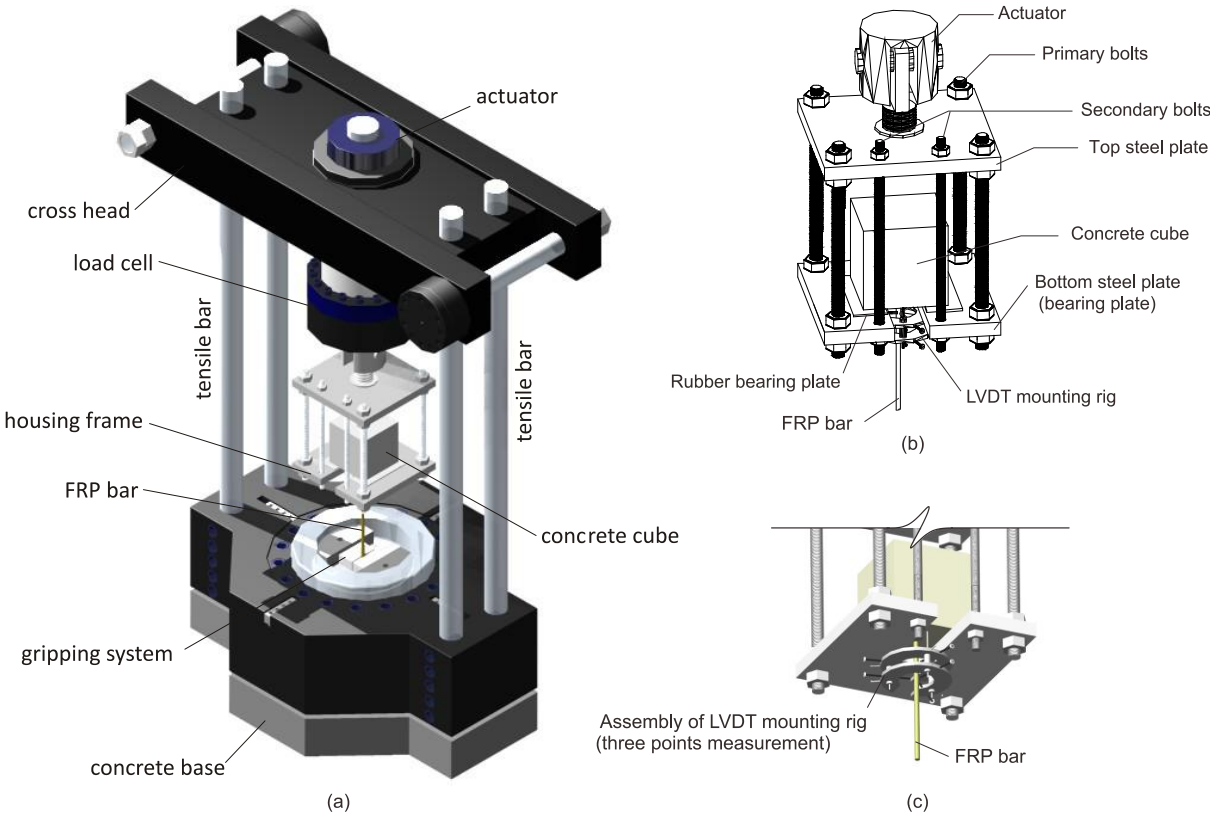

Fig. 9. Pull-out test according to EN 10080 [60]: (a) schematic view, (b) components, and (c) LVDT assembly to measure the bond slip of bars.

4.2 Beam-end test

The beam bond test is included in EN 10080 [63], as shown in **Figs. 10a-b**. In this method, the beam is made up of two symmetrical concrete blocks joined at the centre by a knee-joint at the top and an embedded bar at the bottom. The blocks measure 100 × 200 mm in cross-section, with a 820 mm length. To prevent premature rupture of the concrete in the centrally loaded edge zone, the bar in the non-tested block remains unbonded for a length of 50 mm. The embedment length in this non-tested block remains fixed at 335 mm for all specimens. In contrast, in the tested block, the bar is unbonded for 150 mm, with an embedment length of five times the bar diameter, while the remaining free end of the bar remains unbonded. Beam end tests are generally considered more representative of the stress state in RC members as the applied load induces compression in concrete and tension in the reinforcement bars. However, a primary limitation of this test is that the amount of reinforcement required to prevent shear failure may suppress bond splitting failures [64], which often dominate bond behaviour in actual structures due to the use of thin concrete covers. Additionally, since flexural (i.e. vertical) cracks do not typically develop within the embedded length of the bar, the test conditions may not fully replicate the actual behaviour of RC members.

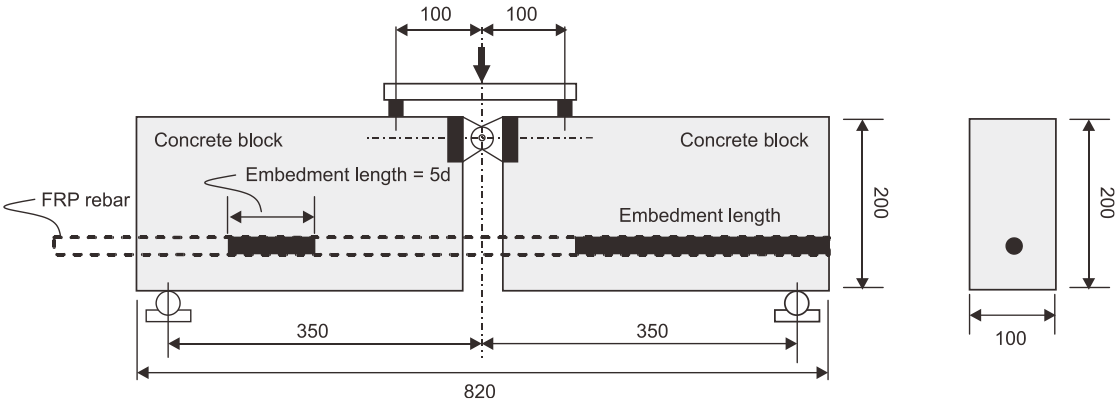

Fig. 10. Beam end test setup for FRP bar to concrete according to EN 10080 [63]. (unit in mm).

4.3 Splice beam test

As stated by the ACI Committee 408 [64], splice beam specimens can be utilised to assess the development of splice bond strength in reinforcing bars. The experimental testing of these splice beams is conducted using a four-point flexural test setup. To calculate the stress in the primary flexural reinforcement, a cracked section analysis can be used. Alternatively, strain gauges can be directly glued onto the surface of the reinforcement, as shown in previous studies on lap spliced beams [65-70]. These tests are often carried out on "long splices" (i.e. a splice longer than five times the bar diameter), thus providing a better representation of the actual average bond stresses expected in actual structures. Moreover, beam splice tests are convenient as these allow for the use of lateral confinement in the lap spliced region, which can be necessary to increase bond strength.

4.4 Comparison of results and guidelines on bond strength

Table 2. Comparison of bond strength across different test methods

Test method	Bond strength in NAC (MPa)	Bond strength in RAC (MPa)	Bond strength in FRP reinforced RAC (MPa)	Observed trend
Pull-out test	10.5-12.3	9.8-11.5	8.1-10.0	Low and not suitable for design
Beam-end test	12.8-14.6	11.2-13.0	9.5-11.3	High but affected by confinement
Splice test	11.2-13.5	10.0-12.2	8.8-10.7	Moderate as this is average bond strength

Table 3. Standard tests to determine bond strength

Test method	Guidelines	Bond strength (τ, τ_u, τ_{max})
Pull-out test	ASTM-C 900-06 [74]	$\frac{F_u}{\pi b_d l}$
	ACI 318-08 [77]	$\frac{\sqrt{f_{ck}}}{d_b}$
	EN 10080:2005 [63]	$\frac{F_u}{5 d_b^2 \pi}$
Beam end test	RILEM 1994 [75]	$\frac{F_u}{\pi d_b l}$
	IS 2770:1967 (RA 2002) [76]	$\frac{F_u}{\pi d_b l}$
Beam splice test	ACI 408R-03 [65]	$\frac{k P_{max}}{40 A_s}$
	ACI 408R-03 [65]	$\frac{A_b f_s}{\pi d_b l}$

Note: τ, τ_u, τ_{max} = bond strength; F_u or P_{max} = pullout load; d_b = diameter of bar; l = bonded/spliced length; σ_s or f_s = stress in steel bar; A_s, A_b = nominal area of a bar; k = constant coefficient (different as per diameter of bar).

Table 2 compares the bond strength across different test methods for both NAC and RAC. Past studies [54] reported that pull-out tests on 100% RAC showed a 10% higher bond strength over NAC. However, other studies [55] indicate that RAC's lower density and increased porosity may negatively affect bonding. This discrepancy arises due to variations in mix design, recycling aggregate conditions, and testing methods. RAC tends to improve bond strength if the recycled aggregate has a rough texture (which enhances mechanical interlock) and/or if saturated surface dry (SSD) conditions exist in the RCA. Past research has also suggested that reducing the diameter of the bars may minimise the impact of the loading rate on bond slip [78]. Understanding these conditions is essential for optimising RAC in case of structural performance.

Table 3 provides various guidelines and standards (including formulas) used to determine bond strength. Based on the test methods examined, it was found the bond strength provided by the beam end test and the splice beam test were somehow similar, thus highlighting the reliability of both methods for assessing bond strength [73].

4.5 Non-destructive evaluation and AI-based prediction models

Whilst traditional bond testing methods provide valuable insights into the interaction between FRP and RAC, emerging non-destructive evaluation (NDE) techniques offer advanced monitoring capabilities, enabling more accurate and real-time bond strength assessments. These techniques reduce specimen damage, enhance long-term monitoring, and improve the reliability of bond strength predictions. Among the prominent NDE methods, acoustic emission (AE) is widely used to monitor micro-crack propagation and bond deterioration in real time [79]. AE sensors detect stress waves generated during loading, providing early indications of failure mechanisms before significant damage occurs. Digital image correlation (DIC) is another effective technique that captures high-resolution images of concrete surfaces to track strain distribution, displacement, and bond-slip behaviour without physical contact [80]. Ultrasonic pulse velocity (UPV) is also employed to assess concrete integrity and bond quality, particularly in detecting internal defects and voids that may affect bonding performance [81]. The use of optical measuring techniques can also offer potential to measure strain distributions (thus bond stresses) over the length of a reinforcing bar [82].

In addition to NDE techniques, AI-based predictive models are gaining attention in bond strength evaluation [83]. Machine learning (ML) algorithms and artificial neural networks (ANNs) analyse experimental datasets to predict bond performance based on variables such as concrete mix composition, aggregate properties, and curing conditions. Finite element modelling (FEM) further aids in simulating bond stress distribution, cracking patterns, and failure mechanisms under various loading conditions [82]. These approaches complement conventional bond testing, improving prediction accuracy while minimising the need for destructive tests, making them valuable tools for future RAC applications.

5 Factors affecting the bond properties of FRP and steel bars in RAC

The bond properties of bars are affected by various factors, including rebar geometry (such as type, anchorage length, rib height, size), concrete properties (such as strength and cover thickness), corrosion effects, confinement, and aggregate characteristics. The subsequent sections outline the key factors influencing bond strength.

5.1 Compressive strength of RAC

Overall, bars embedded in high-strength RAC generally exhibit better bond performance due to improved crack resistance and overall quality. A reduction in pore size and denser concrete packing contribute to enhanced bond strength. However, in high-strength RAC, bond strength development may be slower due to the surface hardness provided by the stronger material. In the case of RAC, bond strength shows a 36% increase compared to NAC [84].

5.2 Effect of recycled aggregates in RAC

The properties of both coarse and fine recycled aggregates can influence the bond strength of FRP, although the results in the literature are inconsistent. RAC containing recycled coarse aggregates

appears exhibiting positive effect on adhesion, showing up to twice the strength observed in NAC due to the high friction developed by the recycled aggregates [85, 86]. However, when aggregate replacement levels are high (approaching 100%), bond strength can decrease by up to 38%, primarily due to increased water absorption, matrix damage, and reduced stiffness in RAC [87, 88]. Recycled fine aggregates exhibit a similar trend, with high-volume replacements resulting in a decrease in bond strength [89, 90]. The inclusion of weld slag as a recycled fine aggregate can increase bond strength by up to 10%, but beyond this point, bond strength starts to decrease. Using recycled rubber or glass aggregates as fine aggregates can improve the strength by about 8%, due to the frictional interaction between cement and reinforcement bars [91]. Incorporating these recycled materials supports circular economy practices in construction by reducing waste, and, if properly processed, they can further enhance bond behaviour. However, careful attention must be paid to the type, grading, and proportion of recycled aggregates to optimise bond strength. Proper surface treatment (e.g. with silica fume) and quality control can be crucial to ensure the effectiveness of RCA when used as replacements for natural aggregates.

5.3 Type of FRP bars

The surface finishing and geometry of FRP bars significantly influences bond strength. **Figs. 11a-f** shows different types of FRP bars with corresponding schematic diagrams, each having unique surface textures for bond enhancement. **Fig 11a** represents a sand-coated or grit-coated FRP bar which improves mechanical interlocking with concrete. **Fig 11b** shows a smooth FRP bar with no additional surface modifications, which may have lower bond strength. **Fig 11c** features a ribbed or deformed FRP bar, where protrusions help in mechanical interlocking. **Fig 11d** is a spiral-wrapped FRP bar, increasing frictional resistance. **Fig 11e** depicts an indented or grooved FRP bar designed for better adhesion, and **Fig 11f** presents a fabric wrapped FRP bar, which enhances mechanical anchorage and durability. These variations cater to different structural applications and performance requirements in concrete structures. Notably, the bond strength of ribbed bars has been reported to over 15 MPa, compared to approximately 5 MPa for smooth bars, thanks to the interlocking mechanism of the deformed ribs [92].

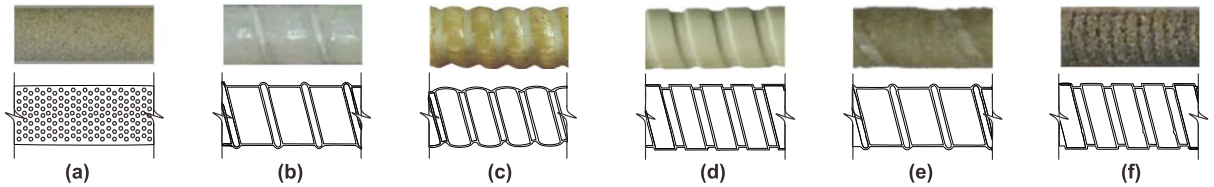

Fig. 11. Different types of FRP bars with coatings: (a) sand coated bar, (b) smooth bar without coating, (c) ribbed bar, (d) spiral wrapped bar, (e) grooved bar, and (f) fabric wrapped bar (adapted from [93]).

5.4 Diameter of FRP bar

The rib geometry and diameter of FRP bars have a significant impact on bond performance. Previous studies have confirmed that as the bar diameter increases, bond strength tends to decrease [94-96]. However, some studies have found that larger diameter bars, due to higher bearing forces, can result in increased bond strength [97, 98]. Additionally, for smaller bars, reduced spacing between the rebar ribs can enhance bond strength [99]. If bond failure is primarily due to pullout, bond strength increases with a greater relative rib area. However, when failure is dominated by splitting, bond strength becomes independent of the bar's rib pattern.

5.5 Effect of bar corrosion

Corrosion of steel bars affects the bond strength in concrete [100]. Corrosion reduces the adhesion between the binder and the rebar, disrupting the forces transferred by bond [101]. Previous studies have shown that the effect of corrosion on bond strength can be either positive or negative, depending on the extent of corrosion [102-104]. At low levels of corrosion (< 6%), the frictional adhesion between steel and concrete can actually enhance bond strength [105, 106]. When comparing the corrosion effects on smooth versus deformed bars, smooth bars tend to perform better due to the frictional roughness developed through corrosion [107]. The use of RAC can marginally increase bond strength as the degree

of corrosion increases (1.6%, 2.6%, and 5.75%), as shown in **Fig. 12a**. This trend suggests that mild corrosion may enhance bond strength due to rust-induced expansion, while excessive corrosion deteriorates the bond strength. **Fig. 12b** presents a corroded reinforcement embedded in concrete with a degree of corrosion 1.6%, displaying significant rust and surface damage. Similarly, **Fig. 12c** illustrates another corroded RAC specimen (with a 2.6% degree of corrosion), emphasising the effect of corrosion on the concrete-reinforcement interface. Due to their non-metallic composition, FRP bars do not experience corrosion, ensuring long-term durability and maintaining bond strength over time, even in aggressive environments. This makes FRP bars a suitable alternative for enhancing the longevity of concrete structures without the degradation associated with corrosion.

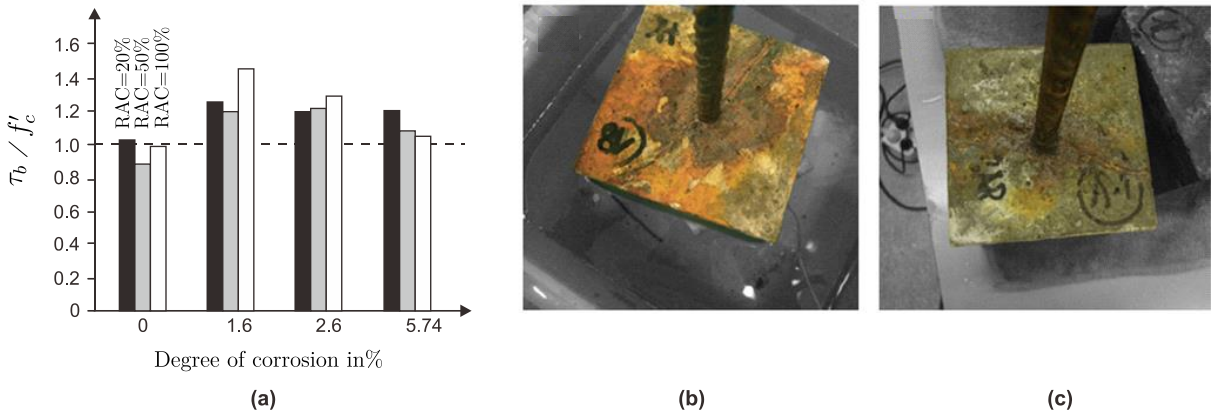

Fig. 12. Bond strength with respect to corrosion degree: (a) degree of corrosion with bond strength, (b) corroded specimen of conventional concrete, and (c) RAC corroded specimen (adapted from [107]).

5.6 Effect of anchorage length

The anchorage length of reinforcing bars plays a crucial role in the development of structural bond strength. Studies have shown that bond strength is inversely proportional to the anchorage length. For example, when comparing a FRP bar with a 5 times diameter length (5Ø) to one with a 10 times diameter length (10Ø), the 10Ø bar exhibits approximately half the bond strength of the 5Ø bar as the stress distributes more uniformly along the length of the bar, thus providing a more “average” bond stress.

5.7 Effect of confinement

The confinement given by stirrups can increase bond strength by about 1.5 times compared to unconfined concrete, owing to the passive confinement effect applied by the stirrups [108]. When lateral stirrups are applied in both vertical and horizontal directions, specimens with confinement show superior bonding compared to those without, often resulting in minimal or no cracks [109-111]. For instance, using a 16 mm main bar with 6 mm stirrup confinement at 75 mm spacing results in a 21.6% improvement in bond strength [112]. Similarly, employing a 20 mm longitudinal rebar with 8 mm stirrup confinement at 100 mm spacing leads to a 34.8% increase in bond strength [113]. External FRP confinement greatly enhances the bond strength of lap-spliced steel bars in beams, improving it by up to 35% [114, 115]. Likewise, active confinement through post-tensioned metal straps can enhance bond strength of lap splices by as much as 50% [116].

5.8 Effect of concrete cover

The concrete cover thickness also contributes to the passive confinement of the bars [117, 118]. Earlier studies have indicated that bond strength can improve by up to 50% when an appropriate concrete cover is used, with the concrete strength and rebar size being key factors influencing this improvement [119]. Additionally, proper cover helps eliminate tensile stresses, reducing crack propagation [120]. **Fig. 13** illustrates the different patterns of splitting cracks in reinforced concrete based on the relationship between reinforcement spacing (C_{si}) and concrete cover (C_b). In **Fig. 13a** the cracks primarily propagate from the reinforcement outward to the concrete surface, indicating that the concrete cover is relatively thin and susceptible to splitting failure. In **Fig. 13b** the cracks form along

the reinforcement direction, showing that when reinforcement is placed closer together relative to the cover thickness, splitting failure tends to occur along the reinforcement rather than outward. The importance of concrete cover in preventing bond failures is acknowledged by current standards, where the effect of transverse steel confinement is incorporated into an equivalent concrete cover for calculating the bonded length of reinforcement bars [121].

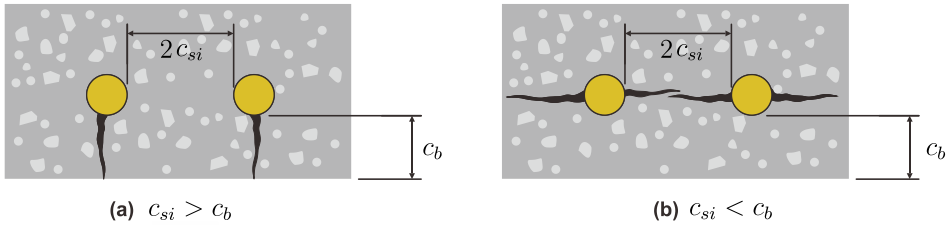

Fig. 13. Possible patterns of splitting cracks in relation to cover thickness.

6 Design equations in code provisions

The key findings from research on bond behaviour have been incorporated into modern design codes. This section highlights the essential design guidelines derived from these findings.

6.1 Eurocode 2 guidelines

6.1.1 Anchorages

The first generation of Eurocode 2 (EC2) [26] provides design values for the ultimate bond stress of steel ribbed bars (f_{bd}), which are applicable for normal-strength NAC.

$$f_{\mathrm{bd}} = 2.25\eta_1\eta_2 f_{\mathrm{ctd}} \tag{1}$$

where f_{ctd} is the design value of concrete tensile strength. The coefficient η_1 considers the quality of bond conditions and the position of the bar during casting. For "good" bond conditions, η_1=1. For poor bond conditions such as bars with more than 300 mm of concrete under them (top bars), the design bond strength is reduced by 30%. η_2 is a coefficient that considers the size of the bar and recognises the fact that larger bars develop lower bond strength. Hence, η_2=1 for bars with $d_{\mathrm{b}} \leq 32$ mm and η_2= (132 - d_{b}) / 100 for bars with $d_{\mathrm{b}} > 32$ mm. The value f_{ctd} can be computed using the values listed in **Table 4,** as per the following expression.

$$f_{\mathrm{ctd}} = \alpha_{\mathrm{ct}} f_{\mathrm{ctk},0.05} / \gamma_c \tag{2}$$

Table 4. Characteristic tensile strength of concrete (MPa)

Variable	Values (MPa)								
f_{ck}	12	16	20	25	30	35	40	45	50
$f_{\mathrm{ctk,\ 0.05}}$	1.1	1.3	1.5	1.8	2.0	2.2	2.5	2.7	2.9

The basic required anchorage length, $l_{\mathrm{b,req}}$, to anchorage a straight bar developing a force $A_s f_{\mathrm{sd}}$ is:

$$/_{\mathrm{ctd}} = \frac{d_b f_{\mathrm{sd}}}{\sigma 4 f_{\mathrm{bd}}} \tag{3}$$

where A_s is the c/s of steel bar, f_{sd} is the design stress of the bar at the position from where the anchorage is measured from, and d_b is the bar size. The design anchorage length, l_{bd}, is:

$$/_{bd} = \alpha_1\alpha_2\alpha_3\alpha_5 /_{b,\mathrm{req}} \geq /_{b,\mathrm{min}} \tag{4}$$

where α_1 considers the bar form, assuming adequate cover, α_2 accounts for the effect of the minimum concrete cover, α_3 considers the confinement provided by transverse reinforcement, α_4 represents the effect of one (or even more) welded transverse bars along l_{bd}, and α_5 represents the impact of pressure applied perpendicular to the plane of splitting along l_{bd}. Note that the product $(\alpha_2\alpha_3\alpha_5) \geq 0.7$. Values for the coefficients α_i are given in **Table 5**. Likewise, $l_{b,min}$ is the minimum anchorage length defined by:

a) for anchorages in tension:

$$/_{b,\min} > \max\left(0.3/_{b,\mathrm{req}}; 10d_b; 100\mathrm{mm}\right) \quad (5)$$

b) for anchorages in compression:

$$/_{b,\min} > \max\left(0.6/_{b,\mathrm{req}}; 10d_b; 100\mathrm{mm}\right) \quad (6)$$

Figs. 14a-c illustrate the different concrete covers (c_d) for different reinforcement configurations in beams and slabs. In **Fig. 14a**, for straight bars, the anchorage depth is calculated as the minimum of half the bar spacing (*a/2*) and the concrete cover thickness (*c*, c_1) which ensures sufficient bond strength. **Fig. 14b** is for bent or hooked bars, the anchorage depth is calculated as the minimum of half the bar spacing (*a/2*) as the bent shape which enhances the mechanical anchorage. **Fig. 14c** is for looped shaped bars, the anchorage depth is simply defined by the concrete cover thickness, as the looped shape inherently provides a secure anchorage. These design considerations ensure adequate bonding and load transfer between reinforcement and concrete in structural elements.

Table 5. Values of coefficients α_1 to α_5

Influencing factor	Anchorage type	Reinforcement bar in tension
Shape of bars	Straight	$\alpha_1 = 1.0$
	Other than straight	$\alpha_1 = 0.7 if\ cd > 3db(a)$ otherwise $\alpha_1 = 1.0$
Concrete cover	Straight	$\alpha_2 = (1 - 0.15(c_d - d_b))/d_b$ ≥0.70 ≤1.0
	Other than straight	$\alpha_2 = (1 - 0.15(c_d - d_b))/d_b$ $\alpha_2 = 1 - 0.15(c_d - 3d_b)/d_b$ ≥0.70 ≤1.0
Confinement by transverse reinforcement not welded to main reinforcement	All types	$\alpha_3 = 1 - K\lambda(b)$ ≥0.70 ≤1.0
Confinement by welded transverse reinforcement	All types, position and size	$\alpha_4 = 0.7$
Confinement by Transverse Pressure	All types	$\alpha_5 = 1 - 0.004p(c)$ ≥0.70 ≤1.0

(a) c_d = defined according to **Fig 14**.

(b) K = coefficient that depends on the position of the transverse reinforcement with respect to the main bar, according to **Fig 15**.

A_{st} = area of the transverse reinforcement along l_{bd}

$A_{st,min}$= area of the minimum transverse reinforcement = 0.25A_s for beams, and 0.0 for slabs

A_s = area of a single anchored bar with maximum bar size

(c) p = transverse pressure (at ultimate limit state) acting along l_{bd}.

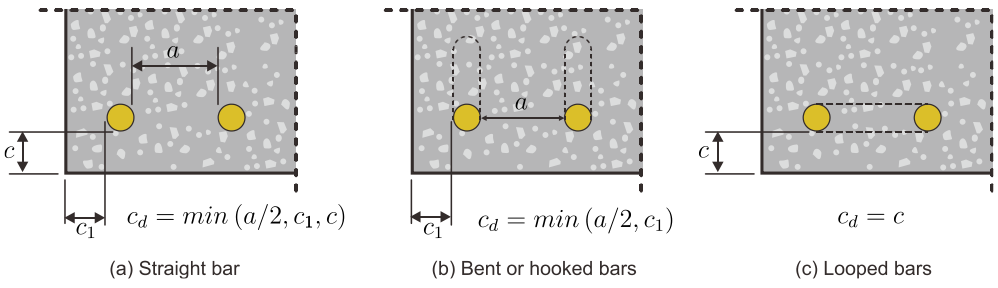

Fig. 14. Values of c_d for straight, bent or hooked, and looped bars.

Fig. 15 illustrates the values of the factor *K* for beams and slabs based on different reinforcement configurations. In **Fig. 15a**, for a beam with an anchored reinforcement bar bent at a right angle, the value of *K* is 0.1, indicating a strong anchorage effect due to the additional confinement provided by

the confinement. **Fig. 15b** is for a slab with a straight reinforcement bar embedded within the concrete, the value of K is 0.05, reflecting a reduced anchorage effect compared to the beam, as there is less confining from the transverse reinforcement. **Fig. 15c** is for a slab where the reinforcement is placed directly at the bottom where K is 0, as there is no significant contribution from the transverse reinforcement to bond strength. These values help in determining the effectiveness of transverse reinforcement in structural design.

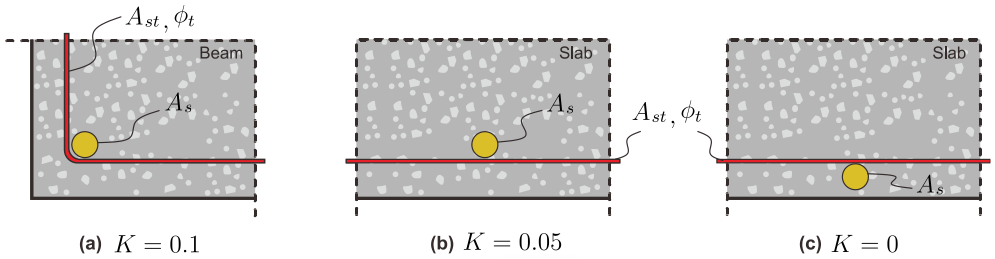

Fig. 15. Values for K for beams and slabs with transverse reinforcement.

6.1.2 Lap splices

Fig. 16 illustrates the concept of lap spliced bars in RC, focusing on the percentage of lapped bars within a specific section. The lapping length (l_o) is the required overlap between two reinforcing bars to ensure proper force transfer. The highlighted areas show the regions where bars are lapped, meaning they are lap spliced to maintain continuity of force transfer. In the considered section, which spans ($0.65l_o$) on either side, different bars are lapped at varying positions, ensuring that not all bars are spliced at the same location. This staggered lap helps in distributing stress more evenly, reducing the risk of weak points in the structure.

EC2 considers that anchorages and lap splices develop different bond strengths. The design lap length is defined as,

$$/_0 = \alpha_1\alpha_2\alpha_3\alpha_5\alpha_6 /_{b,req} \geq /_{0,\min} \tag{7}$$

where:

$/_{0,\min} > \max\left(0.3\alpha_6 /_{b,req}; 15d_b; 200mm\right)$

$\alpha_1, \alpha_2, \alpha_3, \alpha_3$ *and* α_5 are taken from **Table 5**. However, $\Sigma A_{st,min}$ should be taken as $1.0A_s($ σ_{sd}/f_{yd}), with A_s is the area of one lap spliced bar. Likewise, $\alpha_6 = (\rho_1/25)^{0.5}$, but not exceeding 1.5 nor lower than 1.0, ρ_1 is the % of bars lap spliced over $0.65l_0$, measured from the centre of the lap spliced length (**Fig. 16**). The coefficient α_6 can be taken **Table 6**. Intermediate values of α_6 can be calculated by interpolation.

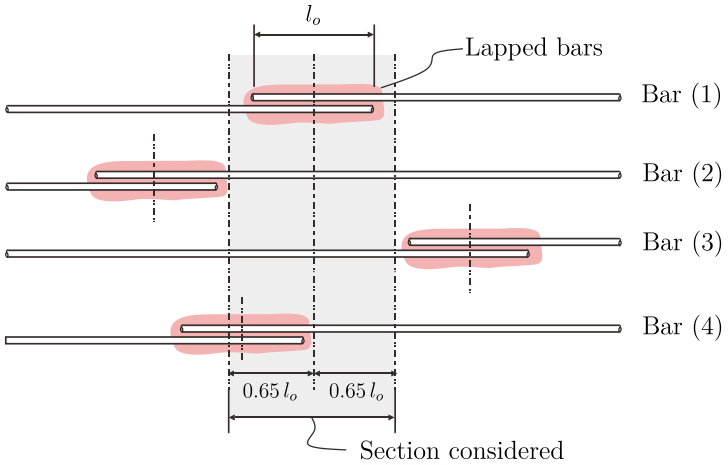

Fig. 16. Percentage of lap spliced bars in one lap section.

Table 6. Coefficient values α_6

Percentage of lap spliced bars relative to total cross-sectional area	α_6
< 25%	1.00
33%	1.15
50%	1.40
>50%	1.50

6.1.3 New Eurocode 2

The informative Annex R of the 2nd generation of EC2 [126] includes a section on bond of FRP reinforcement embedded in NAC. The anchorage length l_{bd} of FRP reinforcement in tension and compression can be calculated as:

$$l_{bd} = k_{1b} \cdot k_{cp} \cdot \phi_f \cdot \left(\frac{\sigma_{ftd}}{217}\right)^{n_\sigma} \cdot \left(\frac{25}{f_{ck}}\right)^{\frac{1}{2}} \cdot \left(\frac{\phi_f}{20}\right)^{\frac{1}{3}} \cdot \left(\frac{1,5.\phi_f}{c_d}\right)^{\frac{1}{2}} \cdot \geq 10\phi_f \quad (8)$$

where k_{lb} is a coefficient depending on the type of load (k_{lb}=50 for persistent and transient design situations, k_{lb}=35 for accidental design situations), k_{cp} is a coefficient accounting for casting effects (k_{cp}=1.0 and 1.2 for bars with "good" and "poor" bond conditions, respectively), ϕ_{f} is the FRP bar diameter, σ_{ftd} is the design value of stress in the FRP reinforcement, f_{ck} is the characteristic compressive strength of concrete, and c_{d} is the concrete cover.

In the above equation, the value of n_σ depends on the stress σ_{ftd}: n_σ = 1.0 for $\sigma_{\mathrm{ftd}} \leq 217$ MPa, and n_σ = 1.5 for σ_{ftd} > 217 MPa. Likewise, the length l_{bd} of the anchorage is limited to:

$$l_{bd} \geq \left(\phi_f / 4\right) \cdot \left(\sigma_{ftd} / f_{bd,100a}\right) \quad (9)$$

where $f_{\mathrm{bd,100a}}$ is the long-term bond strength of FRP reinforcement. Note that $f_{\mathrm{bd,100a}}$ = 1.5 MPa, unless more accurate information is available based on production data.

It should be noted that the above equations are only applicable to NAC and therefore further research should extend their applicability to RAC.

6.2 ACI 318, ACI 440.1R and ACI 440.11

ACI 318 [25] adopts a 'development length' approach, which is based on the "average" bond strength mobilised along the embedded length of the bars. According to the Commentary of the code, a development length is required to avoid "the tendency of highly stressed bars to split relatively thin sections of restraining concrete". No strength reduction factor is included in the expressions used to calculate the development/splice length as the equations allow a strength reduction. The general development length, l_d for deformed bars is defined by:

$$/_d = \left[\frac{x-\mu}{1.1\lambda\sqrt{f_c^{'}}} \frac{\psi_t\psi_e\psi_s}{\frac{c_b - k_{tr}}{d_b}}\right] d_b \quad (10)$$

where ψ_t accounts for the "top bar" effect: if more than 300 mm are casted beneath the development/splice length, $\psi_t = 1.3$, otherwise $\psi_t = 1.0$. The coefficient ψ_e considers the effect of epoxy coating. For epoxy-coated bars or wires with cover less than $3d_b$, or clear spacing less than $6d_b$, $\psi_e = 1.5$. For all other epoxy-coated bars/wires, $\psi_e = 1.2$. For uncoated and galvanised bars, take $\psi_e = 1.0$. The factor ψ_s accounts for the bar size, as smaller diameters tend to exhibit better bond behaviour. For bars with d_b≤19 mm, $\psi_s = 0.8$. For bars with d_b≥22 mm, $\psi_s = 1.0$. The code limits the product of the factor: $\psi_t\psi_e < 1.7$.

The term $(c_{\mathrm{b}} + K_{\mathrm{tr}}) / d_{\mathrm{b}}$ considers the effect of the cover and the contribution of the confinement (assumed as steel) crossing the potential plane of splitting and it is limited to 2.5. The factor K_{tr} is defined by:

$$k_{tr} = \frac{40A_{tr}}{s_{bt}n_b} \tag{11}$$

where A_{tr} represents the cross-sectional area of the transverse confinement, s_{bt} is the spacing between the transverse reinforcement along the development or splice length, and n_b denotes the number of developed or spliced bars along the splitting plane. The code permits the use of K_{tr}=0 as a design simplification, even if transverse confining steel exists.

In North American practice, the bond of FRP reinforcement is often calculated using the ACI 440.1R guidelines [127]. The ACI 440.1R guidelines rely heavily on ACI 318, primarily because many formulas in the former guidelines are extensions (mostly via modification coefficients) of bond equations already developed for steel reinforcement in ACI 318. Accordingly, the development length l_{d} for straight FRP bars is defined as the bonded length necessary to mobilise a stress f_{fr}:

$$\ell_d = \frac{\alpha \dfrac{f_{fr}}{0.83\sqrt{\sigma_c^{'}}} - 340}{13.6 + c/d_b} d_b \tag{12}$$

where α is the "top" bar modification factor, f_{fr} is the FRP bar stress (which depends on the type of failure of the element), f'_c is the concrete compressive strength, *C* is the smallest of the cover to the centre of the bar, or one half of the centre-on-centre of the develop bars, and db is the FRP bar diameter. In the case of lap splices, ACI 440.1R suggests increasing the development length to $1.3l_{\mathrm{d}}$.

As expected, the recently issued design code ACI 440.11-22 [128] adopts a somehow similar approach to ACI 440.1R (i.e. an expression similar to Equation 12) but with some minor modifications. In the first instance, ACI 440.11 is only applicable to GFRP bars. Likewise, the concrete cover thickness C is taken as the smallest of the side concrete cover, the cover over the bar (in both cases measured to the centre of the bar), or one-half of the centre-to-centre spacing of the bars. Moreover, the term C/d_b in the denominator of Equation 13 is limited to 3.5. Likewise, f_{fr} is the stress in the GFRP bar necessary to mobilise the full nominal capacity of the structural element. For lap splices, ACI 440.11-22 provides a classification that depends on the Class type of splice, with the requirements for lap splices Class B being the largest of $1.3l_{\mathrm{d}}$, $20d_b$, or 300 mm as per Table 25.5.2.1 of the same code. Similar to other cases, the equations in ACI 318, ACI 440.1R and ACI 440.11 were developed for NAC.

6.3 Model Code 2010

Model Code 2010 [27] presents one of the most comprehensive guidelines on bond behaviour. The code considers a "design anchorage length" over which bond can be mobilised. As such, the length l_{b} of a reinforcing steel bar is measured to the end of a straight bar or to the outside of a hook or bend. The stress in the reinforcement σ_{sd} to be anchored by bond over the length l_{b} is:

$$\sigma_{sd} = \alpha_1 f_{yd} - \left(F_h / A_{\mathrm{s}}\right) \tag{13}$$

where α_1 is a coefficient that considers the effect of transverse compression on anchorages or lap-splices, f_{yd} is the design yield strength of the reinforcing steel in tension, F_{h} is defined as a force developed by "other measures" such as hooks or bends (F_{h}= 0 in the case of straight bars being pulled in tension), and A_{s} is the area of the bar.

The value of the length l_{b} can be calculated as:

$$l_b = \frac{\phi\sigma_{sd}}{4f_{bd}} \geq l_{b,\min} \tag{14}$$

where ∅ is the bar diameter, and f_{bd} is the design ultimate bond strength. Likewise, the minimum anchorage length is:

$$l_{b,\min} > \max\left\{0.3\phi f_{yd}/\left(4f_{bd}\right); 10\phi; 100\mathrm{mm}\right\} \tag{16}$$

The code includes a series of expressions to calculate the bond strength f_{bd} using a basic bond strength value $f_{bd,0}$.

Model Code 2010 [27] also includes a section on bond of internal FRP reinforcement, but such section redirects the designer to the *fib* Bulletin 40 [129]. The *fib* Bulletin 40 includes bond equations taken from the Canadian Highway Bridge Design Code, Japan Society for Civil Engineering recommendations, and ACI Committee 440, and therefore such equations are applicable only to NAC.

6.4 Proposed modifications expected in future design codes

Current design codes, including ACI 318 [25], Eurocode 2 [26], and the Model Code [27], primarily focus on steel and FRP reinforcement embedded in NAC, with no provisions for reinforcement embedded in RAC. To extend their applicability, several key modifications should be considered in future revisions. Revised coefficients and confinement factors are necessary to reflect the FRP's reliance on adhesion (rather than mechanical interlocking) in RAC, where increased porosity can affect bond strength.

Unlike steel, FRP does not generate significant radial confinement, requiring adjustments to account for its different bond behaviour. Anchorage length modifications should be introduced, as FRP exhibits lower bond-slip resistance than steel. Existing formulas assume steel's ductility, which does not apply to FRP. Future design codes should adopt FRP-specific anchorage models to ensure reliable load transfer. New bond-slip models tailored to FRP reinforced RAC elements should be incorporated. Due to a weaker ITZ in RAC, these models must consider varying aggregate properties, mix design, and moisture conditions to improve bond strength predictions. Bond stress equations in codes should be refined to better represent FRP behaviour in RAC. Implementing these modifications can enhance design accuracy, promoting the sustainable use of RAC with FRP reinforcement.

7 Research trends and future challenges

Most of the existing literature examined bond behaviour in anchorages and splices, and the knowledge gained from these studies is reflected in current guidelines and design codes. Future studies should focus on hybrid composites integrating FRP bars with mineral admixtures to optimise RAC bond performance.

Whilst FRP does not generate significant radial confinement, bond splitting failures have been observed in FRP reinforced RC elements with relatively thin concrete covers. This suggests that confinement could be used to minimise the risk of brittle bond splitting failures. As such, it is expected that future revisions of design codes would develop and integrate appropriate confinement factors for different types of confinement. For instance, passive and active confinement using external FRP jackets or post-tensioned metal straps [115,130,131] could be used to prevent bond failures.

Likewise, it is expected that the use of ML/AI can help develop bond behaviour models for steel and internal FRP reinforcement in RAC structures, as such tools are already being applied to other areas in civil engineering [83,132,133]. Moreover, future research could also use fibre optic sensors [82] to obtain detailed strain distribution profiles along anchored and lap spliced FRP bars in RAC elements.

Other areas for future development in design codes are outlined below:

Recycled Aggregates: The current overestimation of bond strength when using RAC in combination with reinforcing bars should be addressed in design formulas. This would facilitate the acceptance of recycled aggregates as a viable alternative construction material in the industry.

Fibres in Concrete: Incorporating fibres to produce fibre reinforced concrete (FRC) can increase bond strength by up to 1.5 times compared to conventional concrete. Fibres also help reduce crack propagation and enhance the concrete's resistance to corrosion. Therefore, design guidelines should specify the influence of fibres on bond behaviour and consider them as an important factor in determining bond strength.

Corrosion Effects: Corrosion can enhance confinement bonding due to the pressure generated by its expansion mechanism. Therefore, design specifications should include the effects of corrosion, considering its impact on aging, performance, and the durability of concrete structures.

These factors emphasise key areas for future modifications of design codes, ensuring they address emerging materials and elements that influence bond strength and durability in concrete structures.

7.1 Experimental gaps and hybrid reinforcement solutions

Although extensive research has been conducted on RAC and FRP reinforcement separately, experimental gaps remain in understanding their combined behaviour. Long-term durability studies on FRP reinforced RAC elements under cyclic loading, freeze-thaw cycles and chloride penetration are limited. Additionally, bond-slip models (considering both local and average bond stresses) should be refined to consider varying RCA quality, moisture conditions, and FRP surface treatments. Whilst some research has been carried out on structural components made of FRP reinforcement and RAC subjected to high temperature [122, 123], similar full-scale structural investigations on FRP reinforced RAC elements such as beams, slabs, and columns are also lacking. To enhance RAC performance, hybrid reinforcement solutions can also offer promising advancements. Combining FRP with steel reinforcement provides a balance between the FRP's high strength and corrosion resistance and the steel ability to yield. Fibre-reinforced RAC incorporating steel, glass, or basalt fibres improves crack resistance and tensile strength, mitigating bond-related weaknesses [124, 125]. Nano-modified RAC, enhanced with nano-silica or graphene-based additives, reduces porosity and strengthens the ITZ, which can improve bond performance. Addressing these gaps will facilitate the broader adoption of FRP reinforced RAC in structural applications.

8 Conclusions

This article offers a comprehensive review of the bond behaviour between steel and FRP bars and recycled aggregate concrete (RAC) made with recycled concrete aggregate (RCA), examining the various factors that influence bond strength and its characteristics. Several important conclusions can be drawn from the review:

- The presence of porous adhered mortar on the surface of recycled concrete aggregates (RCA) increases water absorption and reduces the bonding capacity of RAC with reinforcement. To minimise these negative effects and improve RAC bonding performance, aggregates should be used in a saturated surface dry condition.
- The use of RAC can enhance bond strength when steel bars exhibit some corrosion (up to 5.75%), achieving higher bond strength compared to conventional concrete. The cracking patterns observed in both RAC and normal concrete specimens are similar, featuring horizontal splitting cracks along the splice region and vertical flexural cracks at the ends of the splice.
- Based on past studies, it was found that moderate recycled concrete aggregate (RCA) replacement levels (50% to 75%) can improve the bond strength of bars due to a rougher interfacial transition zone (ITZ). However, high levels of RCA replacement (close to 100%), can reduce bond strength by up to 38%. Further research on RAC is suggested to clarify these observed trends as RAC is a family of materials.
- Overall, the use of pullout tests to examine bond behaviour of FRP bars in RAC is only recommended for comparisons of bond behaviour among different types of bars, or for benchmark testing. The adoption of beam splice tests is recommended as these provide average bond stresses as those expected in actual structures, and they allow for the use of lateral confinement.
- Current design codes primarily focus on steel and FRP reinforcement embedded in NAC, with no provisions for reinforcement embedded in RAC. To extend their applicability, modifications of existing equations should be considered in future revisions. This is necessary as FRP bars rely on adhesion (rather than on mechanical interlocking) to mobilise bond stresses, which in turn is affected by the RAC's higher porosity.

Acknowledgements

This research was funded by National Research Council of Thailand (N42A680074). This work as partially supported by Walailak University under the international research collaboration scheme (contract no. WU-CIA-02002/2025).

Funding Statement

This project was supported by GFRP Kings under the Research & Development Programme, contact no. WUSTP-2025/256.

CRediT authorship contribution statement

Thanongsak Imjai: Investigation, Formal Analysis, Writing – Original Draft, Conceptualization, Funding Acquisition, Supervision, **Hongguang Wang** and **Radhika Sridhar**: Investigation. **U. Johnson Alengaram**: Supervision, Review & Editing. **Reyes Garcia:** Investigation, Formal Analysis, Writing – Original Draft, Conceptualization, Supervision, Writing – Review & Editing. **Radhakrishna G Pillai**: Investigation, Supervision, Writing – Review & Editing.

Conflicts of Interest

The authors declare that they have no conflicts of interest to report regarding the present study.

References

[1] Pierrehumbert R. There is no Plan B for dealing with the climate crisis. Bull. At. Sci. 2019; 75(5): 215–221. https://doi.org/10.1080/00963402.2019.1654255.

[2] Hu S, Zhang Y, Yang Z, Yan D, Jiang Y. Challenges and opportunities for carbon neutrality in China's building sector—Modelling and data. Build. Simul. 2022; 15(11): 1899–1921. https://doi.org/10.1007/s12273-022-0912-1.

[3] Neupane P, Imjai T, Makul N, Garcia R, Kim B, Chaudhary S. Use of recycled aggregate concrete in structural members: A state-of-the-art review with focus on Southeast Asia. J. Asian Architect. Build. Eng. 2023. https://doi.org/10.1080/13467581.2023.2270029.

[4] Walberg D. Solid and timber construction in residential buildings / Massiv- und Holzbau bei Wohngebäuden. Mauerwerk 2016; 20(1): 16–31. https://doi.org/10.1002/dama.201600685.

[5] Wang B, Yan L, Fu Q, Kasal B. A Comprehensive Review on Recycled Aggregate and Recycled Aggregate Concrete. Resour. Conserv. Recycl. 2021; 171: 105565. https://doi.org/10.1016/j.resconrec.2021.105565.

[6] Ginga CP, Ongpeng JMC, Daly MKM. Circular economy on construction and demolition waste: A literature review on material recovery and production. Materials (Basel) 2020; 13(13): 1–18. https://doi.org/10.3390/ma13132970.

[7] Nunes KRA, Mahler CF. Comparison of construction and demolition waste management between Brazil, European Union and USA. Waste Manag. Res. 2020; 38(4): 415–422. https://doi.org/10.1177/0734242X20902814.

[8] Kabirifar K, Mojtahedi M, Wang C, Tam VWY. Construction and demolition waste management contributing factors coupled with reduce, reuse, and recycle strategies for effective waste management: A review. J. Clean. Prod. 2020; 263: 121265. https://doi.org/10.1016/j.jclepro.2020.121265.

[9] Zheng L, Wu H, Zhang H, Duan H, Wang J, Jiang W, Dong B, Liu G, Zuo J, Song Q. Characterizing the generation and flows of construction and demolition waste in China. Constr. Build. Mater. 2017; 136: 405–413. https://doi.org/10.1016/j.conbuildmat.2017.01.055.

[10] Hossain MU, Poon CS, Lo IMC, Cheng JCP. Comparative environmental evaluation of aggregate production from recycled waste materials and virgin sources by LCA. Resour. Conserv. Recycl. 2016; 109: 67–77. https://doi.org/10.1016/j.resconrec.2016.02.009.

[11] Mo KH, Goh SH, Alengaram UJ, Visintin P, Jumaat MZ. Mechanical, toughness, bond and durability-related properties of lightweight concrete reinforced with steel fibres. Mater. Struct. 2017; 50(1): 1–14. https://doi.org/10.1617/s11527-016-0934-1.

[12] Yang H, Hou Y, Li Z. Bond strength theory between rebar and recycled aggregate concrete after freeze-thaw cycles under stress state I: Uniaxial lateral compression. Constr. Build. Mater. 2024; 411: 134391. https://doi.org/10.1016/j.conbuildmat.2023.134391.

[13] Ganesan N, Indira PV, Sabeena MV. Bond stress slip response of bars embedded in hybrid fibre reinforced high performance concrete. Constr. Build. Mater. 2014; 50: 108–115. https://doi.org/10.1016/j.c onbuildmat.2013.09.032.

[14] Prince MJR, Singh B. Bond behaviour of deformed steel bars embedded in recycled aggregate concrete. Constr. Build. Mater. 2013; 49: 852–862. https://doi.org/10.1016/j.conbuildmat.2013.08.031.

[15] Huang L, Chi Y, Xu L, Chen P, Zhang A. Local bond performance of rebar embedded in steel-polypropylene hybrid fiber reinforced concrete under monotonic and cyclic loading. Constr. Build. Mater. 2016; 103: 77–

92. https://doi.org/10.1016/j.conbuildmat.2015.11.040.
[16] Tepfers R. Cracking of Concrete Cover Along Anchored Deformed Reinforcing Bars. Mag. Concr. Res. 1979; 31(106): 3–12. https://doi.org/10.1680/macr.1979.31.106.3.
[17] Tepfers R, Olsson P-A. Ring Test for Evaluation of Bond Properties of Reinforcing Bars. In: Proceedings of the International Conference: Bond in Concrete - From Research to Practice; 1992; Riga, Latvia: 1–89.
[18] Tufekci MM, Çakır O. An Investigation on Mechanical and Physical Properties of Recycled Coarse Aggregate (RCA) Concrete with GGBFS. Int. J. Civ. Eng. 2017; 15(4): 549–563. https://doi.org/10.1007/s40999-017-0167-x.
[19] Rockson C, Tamanna K, Shahria Alam M, Rteil A. Effect of rebar embedment length on the bond behaviour of commercially produced recycled concrete using beam-end specimens. Constr. Build. Mater. 2021; 286: 122957. https://doi.org/10.1016/j.conbuildmat.2021.122957.
[20] Butler L, West JS, Tighe SL. The effect of recycled concrete aggregate properties on the bond strength between RCA concrete and steel reinforcement. Cem. Concr. Res. 2011; 41(10): 1037–1049. https://doi.org/10.1016/j.cemconres.2011.06.004.
[21] Alhawat M, Ashour A. Bond strength between corroded steel reinforcement and recycled aggregate concrete. Structures 2019; 19: 369–385. https://doi.org/10.1016/j.istruc.2019.02.001.
[22] Kim SW, Do Yun H. Influence of recycled coarse aggregates on the bond behaviour of deformed bars in concrete. Eng. Struct. 2013; 48: 133–143. https://doi.org/10.1016/j.engstruct.2012.10.009.
[23] Shunmuga Vembu PR, Ammasi AK. A Comprehensive Review on the Factors Affecting Bond Strength in Concrete. Buildings 2023; 13(3): 577. https://doi.org/10.3390/buildings13030577.
[24] Behera M, Bhattacharyya SK, Minocha AK, Deoliya R, Maiti S. Recycled aggregate from C&D waste & its use in concrete - A breakthrough towards sustainability in construction sector: A review. Constr. Build. Mater. 2014; 68: 501–516. https://doi.org/10.1016/j.conbuildmat.2014.07.003.
[25] ACI 318-19. Building code requirements for structural concrete. American Concrete Institute, Farmington Hills, MI, USA.
[26] CEN. EN 1992-1-1:2004 Eurocode 2: Design of concrete structures - Part 1-1: General rules and rules for buildings, 2002, European Committee for Standardisation, Brussels, Belgium.
[27] International Federation for Structural Concrete (*fib*), Model Code for Concrete Structures 2010. 2013, 1st Edn. Ernst & Sohn GmbH & Co, Berlin.
[28] Seara-Paz SS, González-Fonteboa B, Eiras-López JE, Herrador MF. Bond behaviour between steel reinforcement and recycled concrete. Mater. Struct. 2014; 47(1–2): 323–334. https://doi.org/10.1617/ s11527-013-0063-z.
[29] Jalilifar H, Sajedi F. Micro-structural Analysis of Recycled Concretes Made with Recycled Coarse Concrete Aggregates. Constr. Build. Mater. 2021; 267: 121041. https://doi.org/10.1016/j.conbuildmat.2020.121041.
[30] Verian KP, Ashraf W, Cao Y. Properties of recycled concrete aggregate and their influence in new concrete production. Resour. Conserv. Recycl. 2018; 133: 30–49. https://doi.org/10.1016/j.resconrec.2018.02.005.
[31] Shi C, Li Y, Zhang J, Li W, Chong L, Xie Z. Performance enhancement of recycled concrete aggregate - A review. J. Clean. Prod. 2016; 112: 466–472. https://doi.org/10.1016/j.jclepro.2015.08.057.
[32] Liang C, Pan B, Ma Z, He Z, Duan Z. Utilization of CO2 curing to enhance the properties of recycled aggregate and prepared concrete: A review. Cem. Concr. Compos. 2020; 105: 103446. https://doi.org/10.1016/j.cemconcomp.2019.103446.
[33] Tam VWY, Wattage H, Le KN, Buteraa A, Soomro M. Methods to improve microstructural properties of recycled concrete aggregate: A critical review. Constr. Build. Mater. 2021; 270: 121490. https://doi.org/10.1016/j.conbuildmat.2020.121490.
[34] Liang C, Cai Z, Wu H, Xiao J, Zhang Y, Ma Z. Chloride transport and induced steel corrosion in recycled aggregate concrete: A review. Constr. Build. Mater. 2021; 282: 122547. https://doi.org/10.1016/j.conbuildmat.2021.122547.
[35] Pepe M, Toledo Filho RD, Koenders EAB, Martinelli E. Alternative processing procedures for recycled aggregates in structural concrete. Constr. Build. Mater. 2014; 69: 124–132. https://doi.org/10.1016/j.conbuildmat.2014.06.084.
[36] Gao C, Huang L, Yan L, Jin R, Kasal B. Strength and ductility improvement of recycled aggregate concrete by polyester FRP-PVC tube confinement. Compos. Part B Eng. 2019; 162: 178–197. https://doi.org/10.1016/j.compositesb.2018.10.102.
[37] Gao Y, De Schutter G, Ye G, Huang H, Tan Z, Wu K. Porosity characterization of ITZ in cementitious composites: Concentric expansion and overflow criterion. Constr. Build. Mater. 2013; 38: 1051–1057. https://doi.org/10.1016/j.conbuildmat.2012.09.047.
[38] Thomas J, Thaickavil NN, Wilson PM. Strength and durability of concrete containing recycled concrete

aggregates. J. Build. Eng. 2018; 19: 349–365. https://doi.org/10.1016/j.jobe.2018.05.007.
[39] Park W, Noguchi T. Influence of metal impurity on recycled aggregate concrete and inspection method for aluminum impurity. Constr. Build. Mater. 2013; 40: 1174–1183. https://doi.org/10.1016/j.conb uildmat. 2012 .03.009.
[40] Xiao J. Recycled aggregate concrete. In: recycled aggregate concrete structures. Springer Tracts in Civil Engineering. Springer; 2018. p. 65–90. https://doi.org/10.1007/978-3-662-53987-3_4.
[41] Lotfi S, Deja J, Rem P, Mróz R, Van Roekel E, Van Der Stelt H. Mechanical recycling of EOL concrete into high-grade aggregates. Resour. Conserv. Recycl. 2014; 87: 117–125. https://doi.org/10.1016/j.resconre c.201 4.03.010.
[42] Kurda R, de Brito J, Silvestre JD. Influence of recycled aggregates and high contents of fly ash on concrete fresh properties. Cem. Concr. Compos. 2017; 84: 198–213. https://doi.org/10.1016/j.cemco ncomp.2017.09. 009.
[43] Wagih AM, El-Karmoty HZ, Ebid M, Okba SH. Recycled construction and demolition concrete waste as aggregate for structural concrete. HBRC J. 2013; 9(3): 193–200. https://doi.org/10.1016/j.hbrcj.2013.08.007.
[44] Guo H, Shi C, Guan X, Zhu J, Ding Y, Ling TC, Zhang H, Wang Y. Durability of recycled aggregate concrete – A review. Cem. Concr. Compos. 2018; 89: 251–259. https://doi.org/10.1016/j.cemconcomp.2018.03.008.
[45] Chen GM, He YH, Jiang T, Lin CJ. Behaviour of CFRP-confined recycled aggregate concrete under axial compression. Constr. Build. Mater. 2016; 111: 85–97. https://doi.org/10.1016/j.conbuildmat.2016.01.054.
[46] Dimitriou G, Savva P, Petrou MF. Enhancing mechanical and durability properties of recycled aggregate concrete. Constr. Build. Mater. 2018; 158: 228–235. https://doi.org/10.1016/j.conbuildmat.2017.09.137.
[47] Gesoglu M, Güneyisi E, Öz HO, Taha I, Yasemin MT. Failure characteristics of self-compacting concretes made with recycled aggregates. Constr. Build. Mater. 2015; 98: 334–344. https://doi.org/10.1016/j.conbuild mat.2015.08.036.
[48] Bao Z, Lee WMW, Lu W. Implementing on-site construction waste recycling in Hong Kong: Barriers and facilitators. Sci. Total Environ. 2020; 747: 141091. https://doi.org/10.1016/j.scitotenv.2020.141091.
[49] Liu J, Yi Y, Wang X. Exploring factors influencing construction waste reduction: A structural equation modeling approach. J. Clean. Prod. 2020; 276: 123185. https://doi.org/10.1016/j.jclepro.2020.123185.
[50] Aslam MS, Huang B, Cui L. Review of construction and demolition waste management in China and USA. J. Environ. Manage. 2020; 264(March): 110445. https://doi.org/10.1016/j.jenvman.2020.110445.
[51] Wu Z, Yu ATW, Shen L. Investigating the determinants of contractor's construction and demolition waste management behaviour in Mainland China. Waste Manag. 2017; 60: 290–300. https://doi.org/10.1016/j.was man.2016.09.001.
[52] Chi B, Lu W, Ye M, Bao Z, Zhang X. Construction waste minimization in green building: A comparative analysis of LEED-NC 2009 certified projects in the US and China. J. Clean. Prod. 2020; 256: 120749. https: //doi.org/10.1016/j.jclepro.2020.120749.
[53] Imjai T, Garcia R, Kim B, Hansapinyo C, Sukontasukkul P. Serviceability behaviour of FRP-reinforced slatted slabs made of high-content recycled aggregate concrete. Structures, 2023, 51; 1071-1082. https://doi. org/10.1016/j.istruc.2023.03.075.
[54] Leelatanon S, Imjai T, Setkit M, Garcia R, Kim B. Punching shear capacity of recycled aggregate concrete slabs. Buildings. 2022, 12(10):1584. https://doi.org/10.3390/buildings12101584.
[55] Pandurangan K, Dayanithy A, Om Prakash S. Influence of treatment methods on the bond strength of recycled aggregate concrete. Constr. Build. Mater. 2016; 120: 212–221. https://doi.org/10.1016/j. conbuildm at.2016.05.093.
[56] Achillides Z, Pilakoutas K. Bond behavior of fiber reinforced polymer bars under direct pullout conditions. J. Compos Constr. 2004; 8(2):173-181. https://doi.org/10.1061/(ASCE)1090-0268(2004)8:2(173).
[57] Gull S, Wani SB, Amin I. The influence of rib configuration on bond strength development between steel and concrete. J. Civ. Eng. Forum 2020; 6(1): 193. https://doi.org/10.22146/jcef.53893.
[58] Seara-Paz SS, González-Fonteboa B, Eiras-López JE, Herrador MF. Bond behaviour between steel reinforcement and recycled concrete. Mater. Struct. 2014; 47(1–2): 323–334. ttps://doi.org/10.16 h17/s11527 -013-0063-z.
[59] Ke L, Li L, Feng Z, Chen Z, Chen G, Li Y. Temperature-dependent bond-slip behavior of CFRP bars embedded in ultrahigh-performance fiber-reinforced concrete. J. Compos Constr. 2024; 28(1): 04023070. ht tps://doi.org/10.1061/JCCOF2.CCENG-4306.
[60] Prince MJR, Singh B. Bond strength of deformed steel bars in high-strength recycled aggregate concrete. Mater. Struct. 2015; 48(12): 3913–3928. https://doi.org/10.1617/s11527-014-0452-y.
[61] Lundgren K, Robuschi S, Zandi K. Methodology for Testing Rebar-Concrete Bond in Specimens from Decommissioned Structures. Int. J. Concr. Struct. Mater. 2019; 13(1). https://doi.org/10.1186/s40069-019-

0350-3.
[62] Prince MJR, Singh B. Bond behaviour of deformed steel bars embedded in recycled aggregate concrete. Constr. Build. Mater. 2013; 49: 852–862. https://doi.org/10.1016/j.conbuildmat.2013.08.031.
[63] BSI, EN 10080; Steel for the Reinforcement of Concrete-Weldable Reinforcing Steel-General. British Standards Institution: London, UK, 2005.
[64] De Almeida Filho FM, El Debs MK, El Debs ALHC. Bond-slip behaviour of self-compacting concrete and vibrated concrete using pull-out and beam tests. Mater. Struct. 2008; 41(6): 1073–1089. https://doi.org/10.1617/s11527-007-9307-0.
[65] ACI 408-03. Bond and Development of Straight Reinforcing Bars in Tension. American Concrete Institute: Farmington Hills, MI, USA; 2003; pp. 1-49.
[66] Gaurav G, Singh B. Experimental investigation for splice strength of deformed steel bars in normal-, medium- and high-strength recycled aggregate concrete. Constr. Build. Mater. 2021; 266: 121185. ttps://doi.org/10.1016/j.conbuildmat.2020.121185.
[67] Garcia R, Helal Y, Pilakoutas K, Guadagnini M. Bond behaviour of substandard splices in RC beams externally confined with CFRP. Constr. Build. Mater. 2014; 50:340-351.
[68] Helal Y, Garcia R, Pilakoutas K, Guadagnini M, Hajirasouliha I. Bond of substandard laps in RC beams retrofitted with post-tensioned metal straps. ACI Struct. J. 2016;113(6):1197-208.
[69] Pandurangan K, Kothandaraman S, Sreedaran D. A study on the bond strength of tension lap splices in self-compacting concrete. Mater. Struct. 2010; 43(8): 1113–1121. https://doi.org/10.1617/s11527-009-9570-3.
[70] Gaurav G, Singh B. Bond strength prediction of tension lap splice for deformed steel bars in recycled aggregate concrete. Mater. Struct. 2017; 50(5): 1–20. https://doi.org/10.1617/s11527-017-1101-z.
[71] Zhao Y, Lin H, Wu K, Jin W. Bond behaviour of normal/recycled concrete and corroded steel bars. Constr. Build. Mater. 2013; 48: 348–359. https://doi.org/10.1016/j.conbuildmat.2013.06.091.
[72] Arezoumandi M, Steele AR, Volz JS. Evaluation of the Bond Strengths Between Concrete and Reinforcement as a Function of Recycled Concrete Aggregate Replacement Level. Structures 2018; 16(July): 73–81. https://doi.org/10.1016/j.istruc.2018.08.012.
[73] Looney TJ, Arezoumandi M, Volz JS, Myers JJ. An Experimental Study on Bond Strength of Reinforcing Steel in Self-Consolidating Concrete. Int. J. Concr. Struct. Mater. 2012; 6(3): 187–197. https://doi.org/10.1007/s40069-012-0017-9.
[74] ASTM C 900-06. Standard test method for pull-out test of hardened concrete. ASTM International Standards 2022; West Conshohocken, PA, United States.
[75] RILEM Technical Recommendations for the Testing and Use of Construction Materials. CRC Press: Boca Raton, FL, USA; 1994. ISBN 9781482271362.IS 2770. Methods of Testing Bond in Reinforced Concrete. Bureau of Indian Standards: New Delhi, India; 1967.
[76] IS 2770. Methods of Testing Bond in Reinforced Concrete. Bureau of Indian Standards: New Delhi, India; 1967.
[77] American Concrete Institute. Building Code Requirements for Structural Concrete (ACI 318-08) and Commentary. American Concrete Institute: Farmington Hills, MI, USA; 2008; Volume 2007. ISBN 9780870312649.
[78] Li X, Wu Z, Zheng J, Alahdal A, Dong W. Effect of loading rate on the bond behaviour of deformed steel bars in concrete subjected to lateral pressure. Mater. Struct. 2016; 49(6): 2097–2111. https://doi.org/10.1617/s11527-015-0636-0.
[79] Ono K. Review on structural health evaluation with acoustic emission. Appl Sci 2018; 8(6): 958. https://doi.org/10.3390/app8060958.
[80] Mousa MA, Yussof MM, Hussein TS, Assi LN, Ghahari S. A digital image correlation technique for laboratory structural tests and applications: A systematic literature review. Sensors 2023; 23(23): 9362. https://doi.org/10.3390/s23239362.
[81] Rehman SKU, Ibrahim Z, Memon SA, Jameel M. Non-destructive test methods for concrete bridges: A review. Constr Build Mater 2016; 107: 58-86. https://doi.org/10.1016/j.conbuildmat.2015.12.011.
[82] Pasityothin I, Thansirichaisree P, Buatik A, Imjai T, Sridhar R, Garcia R, Noguchi T. Strain decay monitoring and analytical prediction of RC columns using Brillouin optical technology and time-dependent deterioration factor. Sensors (Basel, Switzerland) 2025; 25(3): 741. https://doi.org/10.3390/s25030741.
[83] Wattanapanich C, Imjai T, Sridhar R, Garcia R, Thomas BS. Optimizing recycled aggregate concrete for severe conditions through machine learning techniques: A review. Engineered Sci 2024; 31. https://doi.org/10.30919/es1191.
[84] Basaran B, Kalkan I. Investigation on variables affecting bond strength between FRP reinforcing bar and concrete by modified hinged beam tests. Compos. Struct. 2020; 242(March): 112185. https://doi.or g/10. 101

6/j.compstruct.2020.112185.

[85] Lv L, Yang H, Zhang T, Deng Z. Bond behavior between recycled aggregate concrete and deformed bars under uniaxial lateral pressure. Constr. Build. Mater. 2018; 185: 12–19. https://doi.org/10.1016/j.conbuildmat.2018.06.226.

[86] Huang Q, Wang D. Experimental study on bond-slip between steel bar and recycled aggregate concrete. Adv Mater Res 2011; 250–253: 1651–1656. https://doi.org/10.4028/www.scientific.net/AMR.250-253.1651.

[87] Chiriatti L, François P, Mercado-Mendoza H, Apedo KL, Fond C, Feugeas F. Monitoring of the rebar-concrete bond structural health through ultrasonic measurements: application to recycled aggregate concrete. J Civ Struct Heal Monit 2020; 10(4): 595–607. https://doi.org/10.1007/s13349-020-00404-5.

[88] Abed MA, Alkurdi Z, Fořt J, Černý R, Solyom S. Bond Behavior of FRP Bars in Lightweight SCC under Direct Pull-Out Conditions: Experimental and Numerical Investigation. Materials (Basel) 2022; 15(10): 3555. https://doi.org/10.3390/ma15103555.

[89] Pecce M, Ceroni F, Bibbò FA, Acierno S. Steel–concrete bond behaviour of lightweight concrete with expanded polystyrene (EPS). Mater. Struct. 2015; 48(1–2): 139–152. https://doi.org/10.1617/s11527-013-0173-7.

[90] Ananthi A, Karthikeyan J. Combined performance of polypropylene fibre and weld slag in high performance concrete. J Inst Eng Ser A 2017; 98(4): 405–412. https://doi.org/10.1007/s40030-017-0248-5.

[91] Kim SW, Do Yun H. Evaluation of the bond behavior of steel reinforcing bars in recycled fine aggregate concrete. Cem. Concr. Compos. 2014; 46: 8–18. https://doi.org/10.1016/j.cemconcomp.2013.10.013.

[92] Zhang P, Hu Y, Pang Y, Gao D, Xu Q, Zhang S, Sheikh SA. Experimental study on the interfacial bond behavior of FRP plate-high-strength concrete under seawater immersion. Constr. Build. Mater. 2020; 259: 119799. https://doi.org/10.1016/j.conbuildmat.2020.119799.

[93] Wang Y, Wang M, Zhang X, Cai G. Bond of steel-FRP composite bar embedded in FRP-confined concrete: Behavior, mechanism, and strength model. Eng. Struct. 2024; 318: 118693. https://doi.org/10.1016/j.engstruct.2024.118693.

[94] Pop I, De Schutter G, Desnerck P, Szilagy H. Influence of self-compacting concrete fresh properties on bond to reinforcement. Mater. Struct. 2015; 48(6): 1875–1886. https://doi.org/10.1617/s11527-014-0280-0.

[95] Trabacchin G, Sebastian W, Zhang M. Experimental and analytical study of bond between basalt FRP bars and geopolymer concrete. Constr. Build. Mater. 2022; 315(October): 125461. https://doi.org/10.1016/j.conbuildmat.2021.125461.

[96] Law DW, Tang D, Molyneaux TKC, Gravina R. Impact of crack width on bond: Confined and unconfined rebar. Mater. Struct. 2011; 44(7): 1287–1296. https://doi.org/10.1617/s11527-010-9700-y.

[97] Nadir Y, Sujatha A. Bond strength determination between coconut shell aggregate concrete and steel reinforcement by pull-out test. Asian J Civ Eng 2018; 19(6): 713–723. https://doi.org/10.1007/s42107-018-0060-1.

[98] Khaksefidi S, Ghalehnovi M, de Brito J. Bond behaviour of high-strength steel rebars in normal (NSC) and ultra-high performance concrete (UHPC). J. Build. Eng. 2021; 33(July): 101592. https://doi.org/10.1016/j. jobe.2020.101592.

[99] Qi J, Cheng Z, Ma Z, Wang J, Liu J. Bond strength of reinforcing bars in ultra-high performance concrete: Experimental study and fiber–matrix discrete model. Eng. Struct. 2021; 248(October): 113290. https://doi.org/10.1016/j.engstruct.2021.113290.

[100] Fernandez I, Etxeberria M, Marí AR. Ultimate bond strength assessment of uncorroded and corroded reinforced recycled aggregate concretes. Constr. Build. Mater. 2016; 111: 543–555. https://doi.org/10.1016/j.conbuildmat.2016.02.150.

[101] Kusbiantoro A, Nuruddin MF, Shafiq N, Qazi SA. The effect of microwave incinerated rice husk ash on the compressive and bond strength of fly ash based geopolymer concrete. Constr Build Mater 2012; 36: 695–703. https://doi.org/10.1016/j.conbuildmat.2012.06.064.

[102] Coccia S, Imperatore S, Rinaldi Z. Influence of corrosion on the bond strength of steel rebars in concrete. Mater. Struct. 2016; 49(1–2): 537–551. https://doi.org/10.1617/s11527-014-0518-x.

[103] Yalciner H, Eren O, Sensoy S. An experimental study on the bond strength between reinforcement bars and concrete as a function of concrete cover, strength and corrosion level. Cem. Concr. Res. 2012; 42(5): 643–655. https://doi.org/10.1016/j.cemconres.2012.01.003.

[104] Zhu W, Dai JG, Poon CS. Prediction of the bond strength between non-uniformly corroded steel reinforcement and deteriorated concrete. Constr. Build. Mater. 2018; 187: 1267–1276. https://doi.org/10.1016/j.conbuildmat.2018.07.139.

[105] Jiang C, Wu YF, Dai MJ. Degradation of steel-to-concrete bond due to corrosion. Constr. Build. Mater. 2018; 158: 1073–1080. https://doi.org/10.1016/j.conbuildmat.2017.09.142.

[106] Lin H, et al. State-of-the-art review on the bond properties of corroded reinforcing steel bar. Constr. Build. Mater. 2019; 213: 216–233. https://doi.org/10.1016/j.conbuildmat.2019.04.077.
[107] Kim HR, Choi WC, Yoon SC, Noguchi T. Evaluation of Bond Properties of Reinforced Concrete with Corroded Reinforcement by Uniaxial Tension Testing. Int. J. Concr. Struct. Mater. 2016; 10(3): 43–52. https://doi.org/10.1007/s40069-016-0152-9.
[108] Bandelt MJ, Billington SL. Bond behavior of steel reinforcement in high-performance fiber-reinforced cementitious composite flexural members. Mater. Struct. 2016; 49(1–2): 71–86. https://doi.org/10.1617/s11527-014-0475-4.
[109] Li H, Deeks AJ, Su X, Huang D. Tensile bond anchorage properties of Australian 500N steel bars in concrete. J. Cent. South. Univ. 2012; 19(10): 2718–2725. https://doi.org/10.1007/s11771-012-1332-7.
[110] Fang C, Lundgren K, Chen L, Zhu C. Corrosion influence on bond in reinforced concrete. Cem. Concr. Res. 2004; 34(11): 2159–2167. https://doi.org/10.1016/j.cemconres.2004.04.006.
[111] Zheng H, Chen Z, Xu J. Bond behavior of H-shaped steel embedded in recycled aggregate concrete under push-out loads. Int. J. Steel Struct. 2016; 16(2): 347–360. https://doi.org/10.1007/s13296-016-6008-y.
[112] Fawaz G, Murcia-Delso J. Bond behavior of iron-based shape memory alloy reinforcing bars embedded in concrete. Mater. Struct. 2020; 53(5): 1–19. https://doi.org/10.1617/s11527-020-01548-y.
[113] Yang H, Lan W, Qin Y, Wang J. Evaluation of bond performance between deformed bars and recycled aggregate concrete after high temperatures exposure. Constr. Build. Mater. 2016; 112: 885–891. https://doi.org/10.1016/j.conbuildmat.2016.02.220.
[114] Garcia R, Helal Y, Pilakoutas K, Guadagnini M. Bond strength of short lap splices in RC beams confined with steel stirrups or external CFRP. Mater. Struct. 2015; 48: 277–293. https://doi.org/10.1617/s11527-014-0387-3.
[115] Garcia R, Guadagnini M, Pilakoutas K, Pech Poot LA. Fibre-reinforced polymer strengthening of substandard lap-spliced reinforced concrete members: A comprehensive survey. Adv. Struct. Eng. 2017; 20(6): 976–1001. https://doi.org/10.1177/1369433217699632.
[116] Helal Y, Garcia R, Pilakoutas K, Guadagnini M, Hajirasouliha I. Strengthening of short splices in RC beams using Post-Tensioned Metal Straps. Mater. Struct. 2016; 49: 133–147. https://doi.org/10.1617/s11527-015-0602-1.
[117] Akbarzadeh Bengar H, Ahmadi Zarrinkolaei F. Effect of steel fibers and concrete cover on bond behavior between steel deformed bar and concrete under high temperature. Structures 2021; 32(April): 1507–1521. https://doi.org/10.1016/j.istruc.2021.03.062.
[118] Wang H. An analytical study of bond strength associated with splitting of concrete cover. Eng. Struct. 2009; 31(4): 968–975. https://doi.org/10.1016/j.engstruct.2008.12.008.
[119] Liang R, Huang Y, Xu Z. Experimental and analytical investigation of bond behavior of deformed steel bar and ultra high performance concrete. Buildings 2022; 12(4): 1–21. https://doi.org/10.3390/ buildings12040460.
[120] Söylev TA, Franćois R. Effects of bar-placement conditions on steel-concrete bond. Mater. Struct. 2006; 39(2): 211–220. https://doi.org/10.1617/s11527-005-9030-7.
[121] Issa CA, Assaad JJ. Bond of tension bars in underwater concrete: effect of bar diameter and cover. Mater. Struct. 2015; 48(11): 3457–3471. https://doi.org/10.1617/s11527-014-0414-4.
[122] Kefyalew F, Imjai T, Garcia R, Khanh Son N, Chaudhary S. Performance of recycled aggregate concrete composite metal decks under elevated temperatures: a comprehensive review. J. Asian. Archit. Build. Eng. 2024; 1–23. https://doi.org/10.1080/13467581.2024.2309347.
[123] Kefyalew F, Imjai T, Garcia R, Son NK. Fire behavior of high-contents recycled aggregate concrete composite slabs with small openings. Struct. Concr. 2024; 25(6): 4498–4514. https://doi.org/10.1002/suco.202400247.
[124] Leelatanon S, Imjai T, Setkit M, Garcia R, Ma CK. Shear strength of stirrup-free recycled aggregate concrete beams reinforced with steel fibers. Engineered Sci. 2024; 31: 1249. https://doi.org/10.30919/es1323.
[125] Imjai T, Aosai P, Garcia R, Raman SN, Chaudhary S. Deflections of high-content recycled aggregate concrete beams reinforced with GFRP bars and steel fibres. Eng. Struct. 2024; 312: 118247. https://doi.org/10.1016/j.engstruct.2024.118247.
[126] CEN, EN 1992-1-1:2023 Eurocode 2: Design of concrete structures: general rules and rules for buildings, bridges and civil engineering structures, 2023, European Committee for Standardisation, Brussels, Belgium.
[127] ACI Committee 440, ACI-440.1R-15: Guide for the Design and Construction of Structural Concrete Reinforced with FRP Bars, 2015, American Concrete Institute, Farmington Hill, MI, USA.
[128] ACI Committee 440, ACI CODE-440.11-22: Building Code Requirements for Structural Concrete Reinforced with Glass Fiber-Reinforced Polymer (GFRP) Bars—Code and Commentary, 2022, American

Concrete Institute, Farmington Hill, MI, USA.

[129] *fib* Task Group 9.3. *fib* Bulletin 40: FRP Reinforcement in RC Structures. International Federation for Structural Concrete, 2007, pp 1-147

[130] Raffoul S, Escolano-Margarit D, Garcia R, Guadagnini M, Pilakoutas K. Constitutive model for rubberized concrete passively confined with FRP laminates. J. Comp. Constr. 2019; 1;23(6):04019044.

[131] Ma CK, Garcia R, Yung SC, Awang AZ, Omar W, Pilakoutas K. Strengthening of pre-damaged concrete cylinders using post-tensioned steel straps. Proc. Inst. Civ. Eng.: Struct. Build. 2019; 172(10): 703-11.

[132] Sirimewan D, Kunananthaseelan N, Raman S, Garcia R, Arashpour M. Optimizing waste handling with interactive AI: Prompt-guided segmentation of construction and demolition waste using computer vision. Waste Manag. 2024; 15;190: 149-60.

[133] Kargin M, Lukpanov R, Serenkov A, Shaymagambetov Y, Kargin J, Garcia R, Laory I. An innovative structural health assessment tool for existing precast concrete buildings using deep learning methods and thermal infrared satellite imagery. J. Civ. Struct. Health. Monit. 2023; 13(2): 561-78.